J Physiol 587.14 (2009) pp 3539–3559

The Journal of Physiology

Abdominal expiratory activity in the rat brainstem–spinal cord *in situ*: patterns, origins and implications for respiratory rhythm generation

A. P. L. Abdala[1], I. A. Rybak[2], J. C. Smith[3] and J. F. R. Paton[1]

[1]*Department of Physiology and Pharmacology, Bristol Heart Institute, School of Medical Sciences, University of Bristol, Bristol, UK*
[2]*Department of Neurobiology and Anatomy, Drexel University College of Medicine, Philadelphia, PA, USA*
[3]*Cellular and Systems Neurobiology Section, National Institute of Neurological Disorders and Stroke, National Institutes of Health, Bethesda, MD, USA*

We studied respiratory neural activity generated during expiration. Motoneuronal activity was recorded simultaneously from abdominal (AbN), phrenic (PN), hypoglossal (HN) and central vagus nerves from neonatal and juvenile rats *in situ*. During eupnoeic activity, low-amplitude post-inspiratory (post-I) discharge was only present in AbN motor outflow. Expression of AbN late-expiratory (late-E) activity, preceding PN bursts, occurred during hypercapnia. Biphasic expiratory (biphasic-E) activity with pre-inspiratory (pre-I) and post-I discharges occurred only during eucapnic anoxia or hypercapnic anoxia. Late-E activity generated during hypercapnia (7–10% CO_2) was abolished with pontine transections or chemical suppression of retrotrapezoid nucleus/ventrolateral parafacial (RTN/vlPF). AbN late-E activity during hypercapnia is coupled with augmented pre-I discharge in HN, truncated PN burst, and was quiescent during inspiration. Our data suggest that the pons provides a necessary excitatory drive to an additional neural oscillatory mechanism that is only activated under conditions of high respiratory drive to generate late-E activity destined for AbN motoneurones. This mechanism may arise from neurons located in the RTN/vlPF or the latter may relay late-E activity generated elsewhere. We hypothesize that this oscillatory mechanism is not a necessary component of the respiratory central pattern generator but constitutes a defensive mechanism activated under critical metabolic conditions to provide forced expiration and reduced upper airway resistance simultaneously. Possible interactions of this oscillator with components of the brainstem respiratory network are discussed.

(Received 6 December 2008; accepted after revision 26 May 2009; first published online 2 June 2009)
Corresponding author J. F. R. Paton: Department of Physiology and Pharmacology, Bristol Heart Institute, School of Medical Sciences, University of Bristol, Bristol BS8 1TD, UK. Email: julian.f.r.paton@bristol.ac.uk

The eupnoeic pattern of respiration consists of three phases: inspiration, post-inspiration (passive expiration, stage 1) and stage 2 of expiration (Richter, 1982, 1996). During breathing at rest, air is expired passively by recoil forces (see Iscoe, 1998, for review). Augmenting expiratory activity during the second phase of expiration (E2) is always present in the brainstem during eupnoea. Although it is acknowledged that tonic abdominal nerve activity may be present in some species in eupnoea it is probably posture related, and hence non-respiratory (Iscoe, 1998). An expressed phasic expiratory activity in this motor outflow is observed only during increased ventilatory demand, such as during exercise in man (e.g. Abraham *et al.* 2002), hypercapnia or hypoxia in the cat (e.g. Fregosi & Bartlett, 1988; Fregosi, 1994). The specific high-amplitude late-expiratory (late-E) bursts in the abdominal nerve immediately preceding phrenic bursts were also observed in the rat during hypercapnic acidosis and hypoxia (Iizuka & Fregosi, 2007). The origins and mechanisms of generation of this late-E motor activity, and its relation to the normal expiratory activities generated at rest, remain poorly understood and several currently proposed concepts appear controversial.

The Bötzinger complex (BötC), a region located in the rostral part of the ventral respiratory column (VRC) of the medulla oblongata is considered as a primary source of expiratory activity (Cohen, 1979; Ezure, 1990; Jiang & Lipski, 1990; Richter, 1996; Tian *et al.* 1999; Ezure *et al.* 2003). Inhibitory interactions between the BötC expiratory neurones and inspiratory neurones located more caudally in the pre-Bötzinger complex (pre-BötC) and in the rostral part of the ventral respiratory group (rVRG) were proposed as a mechanism for rhythm generation *in vivo* (Cohen, 1979; Ezure, 1990, 2003;

DOI: 10.1113/jphysiol.2008.167502

Jiang & Lipski, 1990; Richter, 1996; Tian *et al.* 1999; Rybak *et al.* 2007; Smith *et al.* 2007). However, two new concepts have emerged that challenge both this view on respiratory rhythm generation and the critical role of BötC in the generation of expiratory activity (Janczewski *et al.* 2002; Feldman & Del Negro, 2006; Janczewski & Feldman, 2006*a*; Onimaru *et al.* 2006). Both concepts were based on so-called '*pre-inspiratory*' activity that was recorded originally in *en bloc in vitro* brainstem–spinal cord preparations of neonatal rats from a region ventral and caudal to the facial nucleus (termed the parafacial respiratory group or pFRG) (Onimaru *et al.* 1987, 1988). The location of the pFRG partially overlaps with the retrotrapezoid nucleus (RTN) and ventrolateral parafacial (vlPF) regions (Fortuna *et al.* 2008). The '*pre-inspiratory*' neurones appear to fire at the very end of expiration. They are inhibited during inspiration and often exhibit a second burst in early post-inspiration. Therefore they have also been termed biphasic expiratory (biphasic-E) neurones (Smith *et al.* 1990, 2000; Ballanyi *et al.* 1994, 1999). Onimaru *et al.* (1987, 1988, 2006) proposed that this '*pre-inspiratory*' (or biphasic-E) activity is generated by a *primary* (pre-inspiratory) oscillator located in the pFRG that entrains a *secondary* (inspiratory) oscillator in the pre-BötC. Others, using both *en bloc in vitro* and *in vivo* preparations of newborn rats, reported that the same biphasic-E activity originating in pFRG drives the activity of abdominal muscles (Janczewski *et al.* 2002). Janczewski & Feldman (2006*b*) using their data obtained from anaesthetized pontine-transected neonatal rats, proposed that the same biphasic-E activity is generated by a separate and independent '*expiratory oscillator*' located in RTN/vlPF, which reciprocally interacts with the pre-BötC inspiratory oscillator, and that the coupling of these two oscillators represents a fundamental mechanism for respiratory rhythm generation (Feldman & Del Negro, 2006; Janczewski & Feldman, 2006*b*). This concept opposes that suggested by Onimaru *et al.* (1987, 1988, 2006).

Relative to other phase-dependent respiratory motor outflows, the abdominal expiratory activity has received little attention in the *in vivo* rat (Iizuka & Fregosi, 2007). Previous studies have not established a clear relationship between ongoing central expiratory activities during normal breathing and the forced expiratory motor activity observed in abdominal nerves under specific conditions. The 'coupled generators' concept of Janczewski & Feldman (2006*a,b*) could only be considered a fundamental mechanism for respiratory rhythm generation if the 'expiratory generator' is critical for (and always operates during) normal breathing (eupnoea) in the juvenile animal. However, Fortuna *et al.* (2008) failed to find rhythmically active biphasic-E neurones in the RTN/vlPF in eupnoeic conditions in anaesthetized adult *in vivo* rats as described previously in *en bloc in vitro* preparations (Onimaru *et al.* 1987, 1988). Instead, they found that certain augmenting expiratory (aug-E) cells in BötC transform to a biphasic-E firing pattern during hypercapnic anoxia. This controversy raises important questions. (1) Is there a separate oscillator that drives AbN motor activity during forced expiration? (2) Does this oscillator operate under eupnoeic conditions and, if so, should it be considered as a necessary component of the respiratory central pattern generator (CPG)? (3) If not, then what are the physiological conditions in which such oscillatory activity emerges? (4) How does this oscillator operate within the brainstem respiratory network and what is the role of other brainstem areas (e.g. pons, BötC) in the generation of forced expiration. And, finally, (5) beyond assisting with expiratory airflow, is there additional physiological relevance for this activity? Thus, we formulated two hypotheses: first, the mechanism(s) generating late-E AbN expiratory activity is not involved in respiratory rhythm generation during eupnoea, but represents an emergent auxiliary mechanism to aid ventilation under specific conditions of enhanced central respiratory drive. Second, late-E activity evoked by drive is generated by a neural population within the RTN/vlPF that requires an excitatory drive from the pons.

In this study, we have tested these hypotheses using *in situ* arterially perfused brainstem–spinal cord rat preparations of juvenile and neonatal rats that allowed us to study the respiratory network under different states: (a) during the generation of eupnoeic-like breathing patterns, but without the depressant effects of anaesthesia or secondary issues of haemorrhage after transection of the neuraxis; (b) in various states of high respiratory drive by manipulation of perfusion gases; and (c) after mechanical (see Smith *et al.* 2007) and chemical removal/inactivation of compartments of the brainstem respiratory pattern generator while recording multiple respiratory motor outputs including AbN as well as central expiratory activity from the BötC.

Methods

In situ arterially perfused brainstem–spinal cord preparation

All procedures conformed to the UK Animals (Home Office Scientific Procedures) Act 1986 and were approved by the University of Bristol ethical review committee. Studies were performed using the *in situ* arterially perfused brainstem–spinal cord preparation of the juvenile and neonatal rats as described previously (Paton, 1996; Paton *et al.* 2006; Pickering & Paton, 2006). In brief, male Wistar rats (60–80 g juvenile rats, or 7- to 10-day-old neonates) were heparinized (1000 units, given I.P.) and subsequently anaesthetized deeply with halothane until loss of their paw withdrawal reflex. Rats were decerebrated pre-collicularly,

and anaesthesia withdrawn. They were then bisected sub-diaphragmatically and the head and thorax immersed in ice-chilled carbogenated Ringer solution. Thoracic phrenic (PN), cervical vagus (cVN), hypoglossal (HN) and thoraco-lumbar (T_9–L_1) abdominal (AbN) nerves were cut distally. Preparations were transferred to a recording chamber. A double lumen catheter (DLR-4, Braintree Scientific, Braintree, MA, USA) was inserted into the descending aorta for retrograde perfusion. Perfusion was supplied via a peristaltic roller pump (Watson Marlow 505D) and consisted of carbogenated Ringer solution at 32°C (for constituents, see below). The second lumen of the catheter was used to monitor aortic perfusion pressure. The baseline perfusate flow was pre-set between 21 and 24 ml min^{-1} (for juvenile rats) and 7–8 ml min^{-1} (for neonates) and adjusted according to the size of the animal. In addition, vasopressin (200–400 pM as required) was added to the perfusate to raise perfusion pressure to between 80 and 90 mmHg (Pickering & Paton, 2006).

Dorsal and ventral exposure of the brainstem

Some preparations were positioned prone and had their head fixed using ear bars and a snout clamp that ensured the brainstem was orientated similarly in all preparations. The cerebellum was removed to gain direct visual access to the dorsal brainstem surface. For exposing the ventral surface of the medulla, some preparations were placed supine and the head fixed on a silicon elastomer cushion using insect pins that ensured the brainstem was orientated similarly in all preparations. The trachea and oesophagus were removed. All muscle and connective tissue covering the basilar surface of the occipital bone were removed. The basilar portion of the atlantooccipital membrane was cut and the bone carefully removed using a micro-Rongeur (Fine Science Tools Inc.) to expose the ventral surface of the medulla from the vertebral arteries to the pontine nuclei.

Stimulation of respiratory network activity

Procedures were used to stimulate AbN expiratory activity or to activate the central respiratory network after transections or microinjections of pharmacological agents. To enhance excitatory drive into the respiratory network the following were performed: (a) activation of the peripheral chemoreceptors by injection of low doses of sodium cyanide (NaCN; 0.03% solution; 25–100 μl bolus) into the aorta; (b) brainstem ischaemia, produced by a transient arrest of the perfusion pump (40–60 s); (c) altering the perfusate gas composition from carbogen (5% CO_2 and 95% O_2) to hypercapnia (7% or 10% CO_2), eucapnic anoxia (5% CO_2 and 95% N_2) or hypercapnic anoxia (7% CO_2 and 95% N_2). A separate reservoir was used for these perfusates which was connected to the main perfusion circuit via a side-tube and 3-way stopcock. All gas compositions were analysed prior to their introduction into the perfusate using a capnograph (Morgan, UK), which was calibrated at least twice daily. All perfusates were gassed for 10 min prior to their introduction to the preparation. Note that the 7% and 10% levels of CO_2 reflect increases of 2% and 5% above eucapnia in the perfused *in situ* preparation.

Electrophysiological recordings

Simultaneous recordings of PN, cVN, HN and AbN motor activities were obtained with bipolar suction electrodes mounted on separate 3-D micromanipulators. We recorded the thoraco-lumbar spinal nerves T_9–L_1 as a measure of peripheral expiratory activity. The lower thoracic nerves T_9–T_{12} innervate mainly expiratory muscles: internal intercostals, external oblique, rectus abdominis and associated muscles. The lower thoraco-abdominal nerves T_{13}–L_1 anatomically and functionally innervate solely expiratory muscles in the abdomen (Iizuka, 2003). In some experiments, we recorded simultaneously both a rostral thoraco-abdominal (T_{10-12}) and a lumbar branch (L_1) of the spinal nerves. In preparations of juvenile rats in which the ventral surface of the medulla was exposed, population and single unit neuronal recordings were made from either the BötC or the RTN/vlPF region with tungsten microelectrodes (1–1.5 MΩ) or glass microelectrodes (filled with 3 M NaCl; 15–20 MΩ), respectively. The latter were used to differentiate between recruitment of cells *versus* increased firing within a single neurone. Microelectrodes were positioned with a 3-D micromanipulator and nanostepper (custom-made) into these brainstem regions under the visual control of a binocular microscope using surface landmarks (trapezoid body, rootlets of the HN, blood vessels) for orientation. The RTN/vlPF region was located 50–100 μm beneath the ventral surface, 0.5 mm caudal to the caudal end of the trapezoid body and 1.7–2 mm lateral from the midline (aligned with the rootlets of the HN). We also determined the BötC by mapping population activity profiles along the rVRG–pre-BötC–BötC column for orientation. In addition, recording sites were marked using electrolytic lesions in some experiments with subsequent histological reconstruction. Nerve and unit recordings were AC amplified (20k) and band-pass filtered (60 Hz to 3 kHz). Nerve and population activity signals were rectified and integrated (50 ms time constant) online (Spike2 software, Cambridge Electronic Design (CED)). All electrophysiological data were digitized (3–10 kHz, CED A/D converter) with Spike2 software and analysed off-line.

Switching from a three-phase to two- and one-phase respiratory oscillations by precise brainstem microtransections

Recently, we showed that the normal three-phase respiratory rhythm can be converted to a two- and one-phase pattern by making precise sequential transverse transections at the ponto-medullary junction and the junction of the BötC and pre-BötC, respectively (Smith *et al.* 2007). To assess the activity pattern of the AbN during both the two- and one-phase respiratory rhythms, we used a custom-made micro-vibratome (Smith *et al.* 2007) to make these sequential transverse sections through the brainstem of the *in situ* juvenile rat preparation while recording respiratory motor outputs. When required, we adjusted the flow rate of the perfusion pump or applied vasopressin to the perfusate to correct for any changes in perfusion pressure caused by the transections. The level of each transverse cut made with the microvibratome was documented *post hoc* by histological reconstruction and related to the changes in motor pattern that we described previously (Smith *et al.* 2007).

Chemical inactivation of the RTN/vlPF region

In preparations of juvenile rats in which the ventral surface of the medulla was exposed, we injected either isoguvacine hydrochloride or vehicle (Ringer solution) bilaterally into the RTN/vlPF region using two single-barrelled glass pipettes (tip diameter 20 μm) mounted in a custom-made twin micropipette holder. The tips of the pipettes were driven 50–100 μm beneath the ventral surface, 0.5 mm caudal to the caudal end of the trapezoid body and 1.7–2 mm lateral from the midline (aligned with the rootlets of the HN). Bilateral microinjections were performed < 60 s apart. We controlled volumes injected (30–60 nl) by observing the displacement of the meniscus using a microscope with a pre-calibrated ocular graticule. At the end of the experiments, we injected equivalent volumes (30–60 nl) of Pontamine Sky Blue (2%) bilaterally to mark microinjection sites. This provided a location of the centre of microinjection, but since diffusion coefficients of the drug and dye may have differed we cannot comment on the degree of effective spread.

Histological reconstruction

The head of the preparation with the transected brainstem *in situ* or marked microinjection or recording sites was fixed in 10% buffered formaldehyde–30% sucrose solution for at least 2 days before the brainstem was removed. Sagittal sections were cut (50 μm thick), mounted onto subbed slides and stained with Neutral Red (1%). This allowed reconstruction of the precise boundaries for the regions generating the different respiratory patterns and mechanisms underpinning the distinct rhythms generated.

Solutions and pharmacological agents

The composition of the Ringer solution was (in mM): NaCl (125); $NaHCO_3$ (24); KCl (3); $CaCl_2$ (2.5); $MgSO_4$ (1.25); KH_2PO_4 (1.25); glucose (10); pH 7.35–7.4 after carbogenation (5% CO_2 and 95% O_2). Osmolality was 290 ± 5 mosmol $(kg\,H_2O)^{-1}$. Polyethylene glycol (MW 20 000; 1%) was added as an oncotic agent. Unless stated, all chemicals were from Sigma-Aldrich (UK). Vecuronium bromide (4 $\mu g\,ml^{-1}$; Organon Teknica, Cambridge, UK) was added to the perfusion solution to block neuromuscular transmission. Isoguvacine hydrochloride, a $GABA_A$ agonist, was prepared fresh daily in Ringer solution (10–20 mM, pH 7.4).

Analysis

For analysis of data we used Spike2 (version 6.8, Cambridge Electronic Design) and a custom-written script for measurement of parameters of motor or population activity (cycle period/frequency, inspiratory duration, expiratory duration, activity amplitude). We averaged all parameters including cycle-triggered averages (CTAs) across at least 50 respiratory cycles. Significance of data was assessed with either a two-tailed Student's *t* test or ANOVA and a *post hoc* Holm-Sidak Test (Sigma Stat, 3.01 Systat Software). All values indicated are the mean $\pm$ standard error of the mean (S.E.M.) and '*n*' is the number of preparations. Differences were considered significant at the 95% confidence limit.

Results

Characterization of abdominal spinal respiratory motor outflow in the rat

Control conditions of eucapnia and normoxia ($n = 10$). The AbN (L_1) exhibited low amplitude post-I discharge only (see Fig. 1*A*, inset a_1, and Fig. 2, left column). The firing patterns of PN, HN and cVN were identical to those described recently (Smith *et al.* 2007). Briefly, and as seen in these figures, under standard conditions (e.g. perfusate gassed with carbogen), PN exhibits a ramp inspiratory discharge pattern that is also present in the cVN. In the cVN, the inspiratory motor activity is followed by a decrementing post-inspiratory discharge that terminates in the middle of expiration. The HN expresses an incrementing inspiratory discharge that often starts slightly before PN discharge.

Switching to various anoxic/hypercapnic conditions. Hypercapnic anoxia, eucapnic anoxia, ischaemia and peripheral chemoreceptor activation evoked an incrementing expiratory discharge in the AbN that peaked at the very end of expiration in both neonates ($n = 3$) and juvenile rats ($n = 10$).

Juvenile rats. In these preparations, eucapnic anoxia (5% CO_2 and 95% N_2) produced an expressed expiratory activity in AbN (Fig. 1*A*, insets a_2–a_4), which was either an incrementing type (insets a_2, a_3), or a biphasic-E discharge (inset a_4). The biphasic-E discharges contained variable relative amplitudes and durations of incrementing expiratory activity and post-I components, and this pattern was unstable over sustained stimulation. In the early stage of eucapnic anoxia (5% CO_2 and 95% N_2), when inspiratory activity (PN) was enhanced, the baseline level of AbN post-I activity was maintained or increased, and incrementing expiratory activity in AbN emerged (Fig. 1*A*, inset a_2). The onset of the AbN incrementing discharge drifted, occurring later in the expiratory period depending on the duration of the stimulation. Later, when respiratory frequency slowed with continued eucapnic anoxia, incrementing AbN bursts (Fig. 1*A*, inset a_3) were observed for 20–30 s before initiation of gasping. During gasping (Fig. 1, inset a_4) the AbN motor output showed biphasic-E bursts featuring incrementing expiratory activity preceding PN burst, quiescence during inspiration (PN discharge), and decrementing post-I activity. The cranial outflows (cVN and HN) during gasping exhibited synchronous decrementing bursts that were phase-locked with the PN discharge, as described previously (Paton *et al.* 2006). In all juvenile rats, sustained eucapnic anoxia resulted in respiratory arrest, which was reversible. Hypercapnic anoxia (7% CO_2 and 95% N_2, not shown) produced very similar patterns of activity to those of eucapnic anoxia. Peripheral chemoreceptor activation also elicited biphasic-E AbN discharges (Fig. 1*C*).

Neonatal rats. These preparations showed a similar eupnoeic respiratory pattern to juvenile rats during eucapnic normoxia (see above and Fig. 1*B*, left column). When exposed to prolonged eucapnic hypoxia (Fig. 1*B*, right column) or hypercapnic hypoxia (not shown), neonates generated gasps which were accompanied by biphasic-E bursts in the AbN. Unlike juvenile animals, neonates could generate multiple gasps accompanied by biphasic-E AbN bursts before respiratory arrest. Compared to juvenile rats, neonates generated many more gasps and the corresponding biphasic-E bursts in the AbN (e.g. $>$ 20 gasps for neonates *versus* $<$ 8 for juvenile).

Hypercapnia-evoked AbN discharge. In both juvenile and neonatal rats, normoxic hypercapnia (7–10% CO_2, balanced with O_2) was the most reproducible stimulus for the generation of persistent incrementing AbN discharges as shown in Fig. 2*A* and *B*. Accordingly, it was used in the remainder of the study for further investigation of AbN expiratory activity.

The incrementing AbN activity generated during prolonged hypercapnia is defined here as a typical late-E burst which is characterized by a sharp onset, incrementing shape and high amplitude. It was initiated during the final one-third of the expiratory period and terminated abruptly at the onset of inspiration recorded from the PN. At the same time, our analysis has shown that the late-E AbN discharge generated during hypercapnia differs from the incrementing AbN output induced by hypoxia (described above) in its temporal relations to the discharges in other nerves (see next section). Since the late-E AbN activity induced by hypercapnia in juvenile and neonatal rats was nearly identical (Fig. 2), the quantitative analysis below and all additional protocols were performed on juvenile rats.

In juvenile rats, late-E bursting could be maintained reliably for repeated bouts of 40–60 min under moderate (7% CO_2) or strong (10% CO_2) hypercapnia without detriment to the respiratory rhythm. We compared this motor AbN activity at spinal levels T_9–L_1. At all spinal levels, AbN presented a qualitatively similar pattern to that described above but the relative amplitudes of post-I *versus* late-E discharges differed between rostral to more caudal segments. During eucapnia, thoracic branches (T_9–T_{12}) exhibited lower amplitude post-I discharge than lower thoraco-lumbar (T_{13}–L_1) AbN nerves (1.26 ± 0.4 *vs.* $3.07 \pm 0.9\ \mu$V, respectively; $P < 0.05$). Additionally, during hypercapnia (7% and 10% CO_2) lumbar AbN nerves exhibited a higher amplitude of late-E expiratory activity than thoracic branches, when recorded simultaneously (8.8 ± 1.6 *vs.* $3.1 \pm 1.2\ \mu$V for 7% CO_2 and 11.1 ± 2.7 *vs.* $3.3 \pm 1.1\ \mu$V for 10% CO_2, $P < 0.01$, respectively). Interestingly, the amplitude of the late-E burst during different levels of hypercapnia (7% and 10% CO_2) was not significantly changed with the intensity of stimulus, behaving as an '*all-or-nothing*' event ($P > 0.05$).

During normoxic hypercapnia at 7% CO_2, late-E AbN bursts sometimes skipped PN cycles (Fig. 2). The regularity of cycles containing late-E bursts was related to the level of hypercapnia ($60 \pm 6\%$ *vs.* $83 \pm 5\%$ of PN cycles at 7% and 10% CO_2, respectively; $P < 0.001$). It was also apparent that in contrast to systemic hypoxia/peripheral chemoreceptor stimulation, the post-I activity in AbN was reduced during hypercapnia (normoxia) relative to control.

Occurrence of late-E AbN discharge is always coupled with specific changes in PN and cranial respiratory motor outflows. Figure 2 shows that when late-E burst activity occurs in AbN (e.g. in 7% CO_2) the timing and shape of the

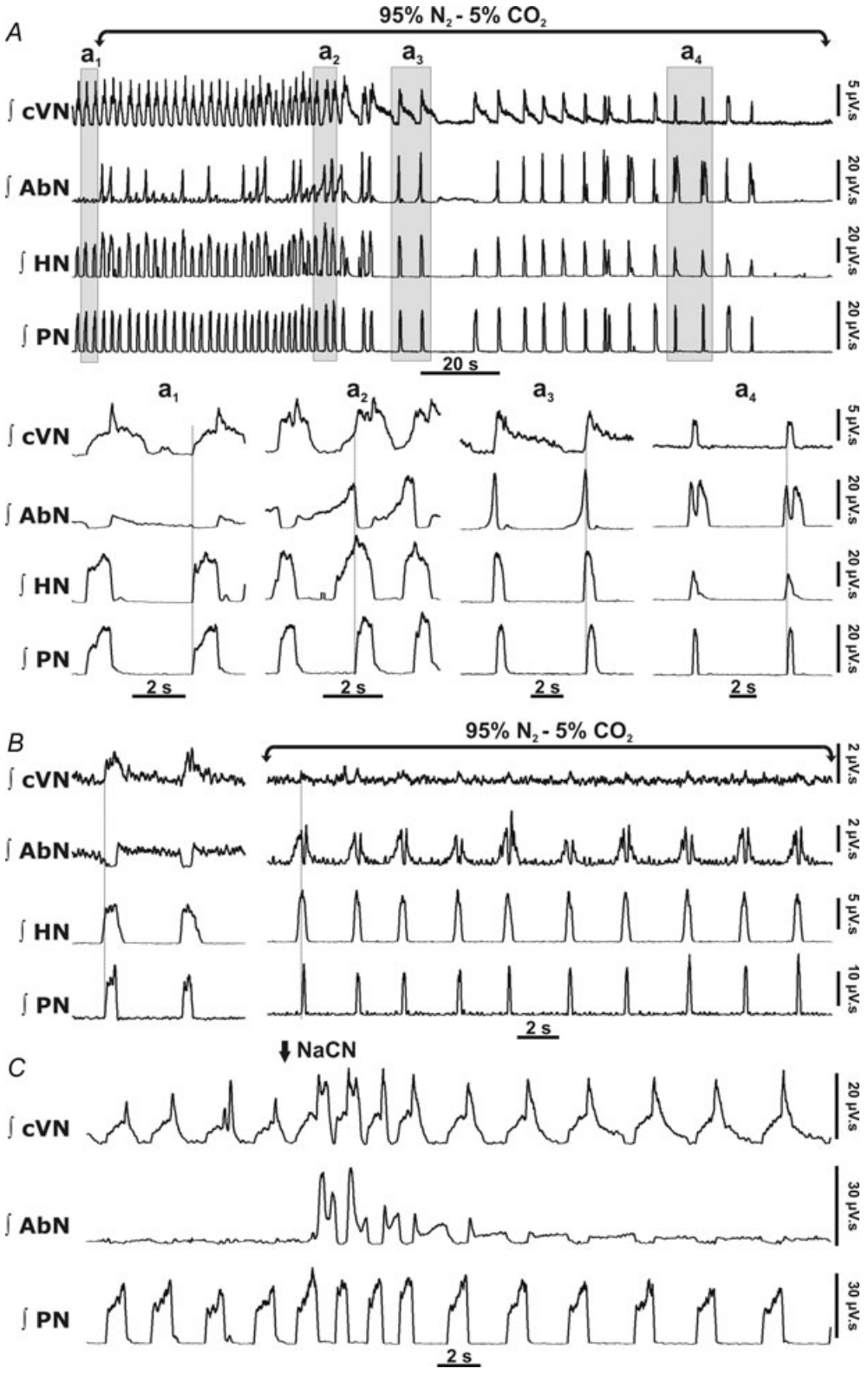

Figure 1. Abdominal motor activity patterns during high central respiratory drive
Effect of increased respiratory drive on integrated phrenic (PN), hypoglossal (HN), lumbar abdominal (AbN) and central vagus (cVN) outflows recorded simultaneously. *A*, during eupnoea in the juvenile rat (a_1) AbN activity exhibits low amplitude post-I discharge. The response to anoxia (95% N_2 and 5% CO_2) was divided into 3 phases: inspiratory excitation (a_2), inspiratory depression (a_3) and gasping (a_4). During phases a_2 and a_3

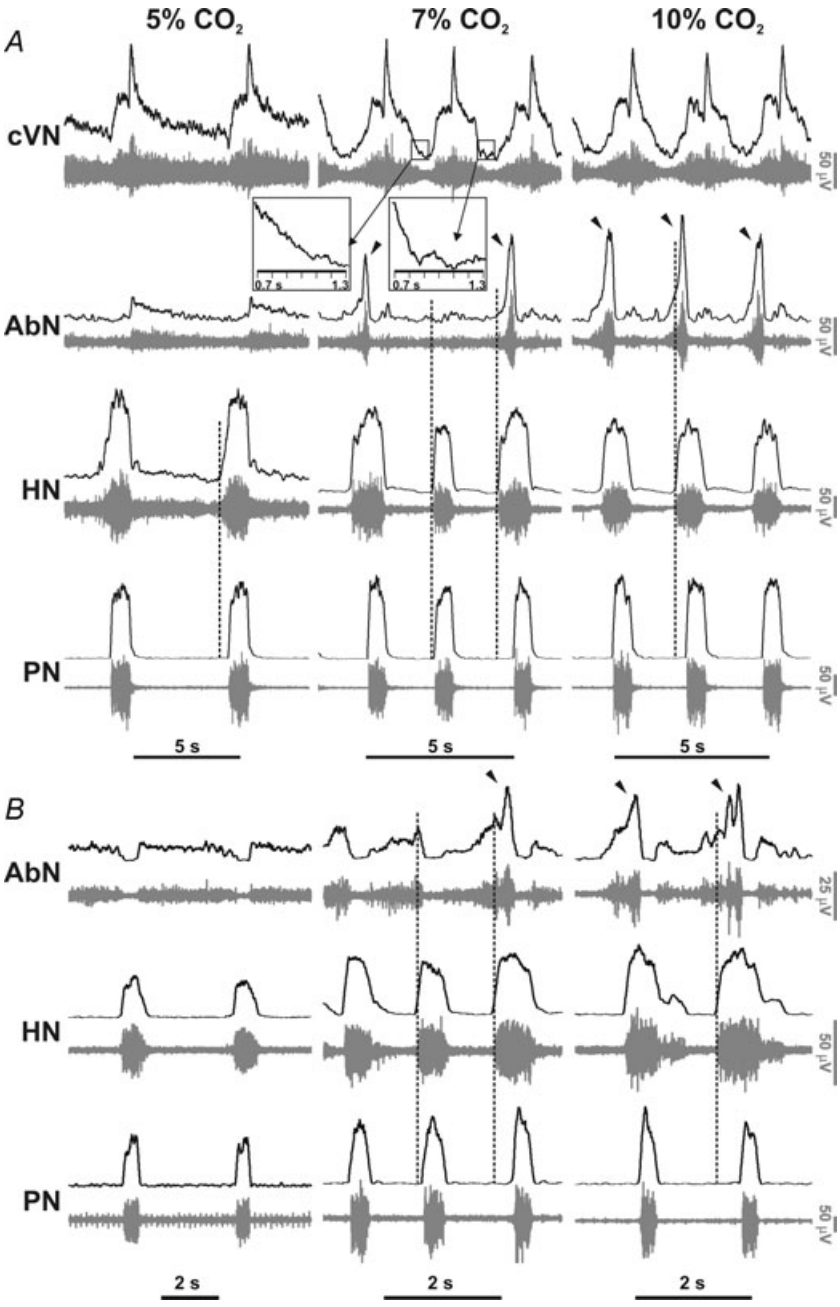

Figure 2. Characteristics of the respiratory abdominal motor outflow in juvenile and neonatal rat *in situ* preparations
Representative activity patterns of phrenic (PN), hypoglossal (HN), lumbar abdominal (AbN) and central vagus (cVN) nerves recorded simultaneously during eupnoea (5% CO_2) and hypercapnia (7%, 10% CO_2) in juvenile (*A*) and neonatal rats (*B*). Raw (grey traces) and integrated (black traces) motor nerve outputs; vertical dashed lines indicate onset of HN bursts. Hypercapnia (7% CO_2) elicited typical AbN late-E bursts (arrowheads) that exhibited cycle-to-cycle 'skipping' but were stable at 10% CO_2. Insets in *A*: late-E AbN bursts were correlated with shorter duration of the preceding cVN post-inspiratory activity (see also Fig. 3*E*). The time scale in the insets indicates time from the end of inspiration in PN.

subsequent PN discharge changes so that: (a) the onset of the following PN burst is delayed resulting in prolongation of the preceding interburst interval in PN (Fig. 3*D*) and (b) the duration of the PN burst is correspondingly reduced (Fig. 3*B*, see also panels *F vs. C*). At the same time, PN amplitude remains unaltered (Fig. 3*E*). Note that the *in situ* preparation normally exhibits an incrementing PN pattern during eucapnia (Fig. 1*A*, inset a_1, Fig. 2). In

augmenting AbN discharge emerged with variable amplitudes. The pattern transformed into biphasic-E AbN activity during gasping (phase a_4). Note that the appearance of a single doublet inspiratory burst (third burst prior to a_4) was predicted by the model of Wittmeier *et al.* (2008). *B*, neonatal rats ($n = 3$) presented similar motor outflows during gasping with biphasic-E AbN discharges. This activity continued longer (in comparison with juvenile rats) without suffering respiratory arrest. *C*, bolus injections of NaCN (100 μl, 0.03%) into the perfusate to activate peripheral chemoreceptors also induced biphasic-E activity in the AbN in juvenile rats.

hypercapnia (7% CO_2) when late-E AbN was absent, PN also exhibited an augmenting pattern comparable to that seen in control conditions (Figs 2 and 3*C*). However, when AbN late-E bursts occurred, the initial part of the following PN burst was 'cut off' in direct relation with AbN late-E activity and hence the PN burst lost the initial incrementing onset (Fig. 3*F*).

The presence of late-E AbN activity was also coupled with differences in cranial motor outflows. Following a late-E burst, the amplitude and duration of the pre-I component of HN discharge increases (see Fig. 4*A*–*C*). As seen in the CTA in Fig. 4*C*, the onset of this HN pre-I activity coincided with the onset of late-E AbN discharge and, hence, occurred earlier and lasted longer. This suggests that the late-E activity correlates with a positive effect on HN activity but a negative effect on PN activity (see above). Likewise, the pre-I activity recorded from the cVN was longer when preceded by a late-E burst in the AbN (Fig. 4*D*–*F*). In contrast, the duration of post-I activity in the cVN was reduced when followed by a late-E AbN burst in 7% CO_2 (insets in Fig. 2 and Fig. 4*E* and *F*).

Under 10% CO_2, nearly all respiratory cycles contained late-E bursts; therefore averages for cycles not containing late-E bursts are not shown. Compared to control (5% CO_2), 10% CO_2 increased PN rate and amplitude (Fig. 3*A* and *D*) but decreased burst duration. In the HN, the burst amplitude (Fig. 4*A*) and the duration of the pre-I component both increased and its onset was advanced (Fig. 4*B*). In the cVN, the duration of post-I activity was reduced (Fig. 4*E*).

In summary, the typical hypercapnia-evoked late-E AbN activity was sustainable, was restricted to the last third of the expiratory phase throughout the stimulus and was always correlated with enhanced pre-inspiratory activity in the HN motor outflow. We have

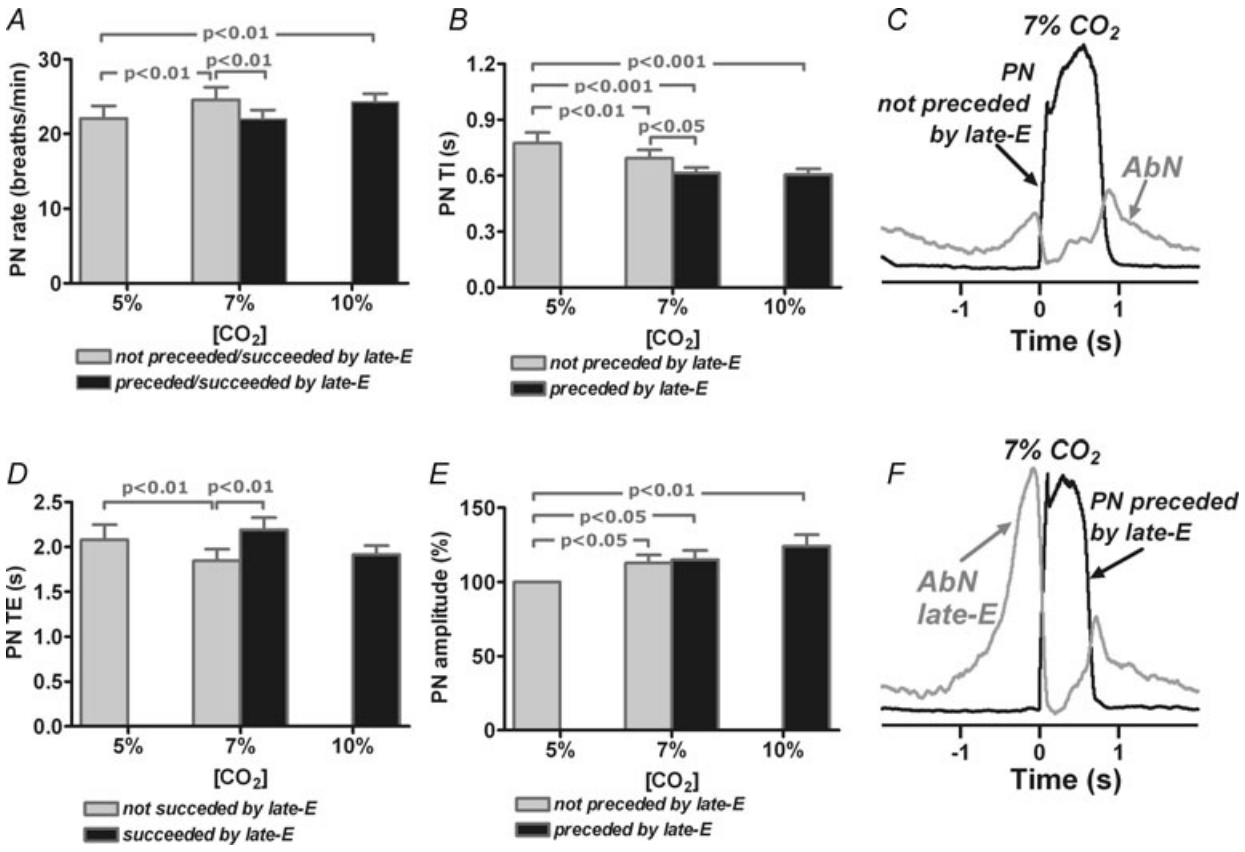

Figure 3. Effect of abdominal late expiratory discharge on phrenic activity
Graphs show phrenic nerve (PN) burst rate (*A*), burst duration (TI) (*B*), inter-burst duration (TE) (*D*) and amplitude (*E*) under eupnoea (5% CO_2) and hypercapnia (7–10% CO_2). We averaged cycles without (grey bars) and with abdominal (AbN) late-E activity (black bars). All values represent mean ± S.E.M. (error bars), $n = 10$. The representative cycle-triggered average (CTA) shows PN bursts not preceded by late-E AbN activity (*C*) under hypercapnia (7% CO_2). CTA in *C* represents 30 cycles not preceded by late-E AbN bursts. The presence of AbN (grey) late-E bursts correlated with shortened duration of succeeding PN bursts (black) and prolonged the PN inter-burst interval without changing its amplitude (*F*). CTA in *F* is an average of 20 cycles preceded by late-E AbN bursts. Time 0 indicates onset of inspiration on PN.

studied the mechanisms and origins of this late-E AbN activity.

Determining critical brainstem structures for expression of late-E AbN

Two methods for defining brainstem regions critical for the expression of late-E AbN activity were employed: micro-transection and microinjection.

Microtransection. Using precise sequential rostro-caudal micro transverse sectioning, we identified medullary compartments of the respiratory network required for the generation of various forms of expiratory activity. After transection at the ponto-medullary junction to remove the pons, the remaining neuraxis spontaneously generated a two-phase (inspiratory–expiratory) rhythmic activity, identified in recordings of PN and cVN. Following transection between the BötC and pre-BötC (Fig. 5), the pattern was converted to a one-phase inspiratory pattern as described previously (Smith *et al.* 2007). The two-phase pattern consisted of phase-locked inspiratory activity in both PN and cVN, both of which exhibited 'square-wave'-shaped bursts. As reported earlier (Smith *et al.* 2007), we found that post-inspiratory activity in cVN was abolished after pontine transection and could not be reinstated by hypercapnia, hypoxia, anoxia, ischaemia or peripheral chemoreceptor activation. This was also found to be the case for the post-inspiratory activity recorded from the AbN (Fig. 5), which was also abolished and did not return even with increasing excitatory drive to the network (10% CO_2). Similarly, ponto-medullary transection abolished the late-E bursts in the AbN: the AbN activity became tonic throughout the expiratory phase, and this pattern was unaffected even after increasing

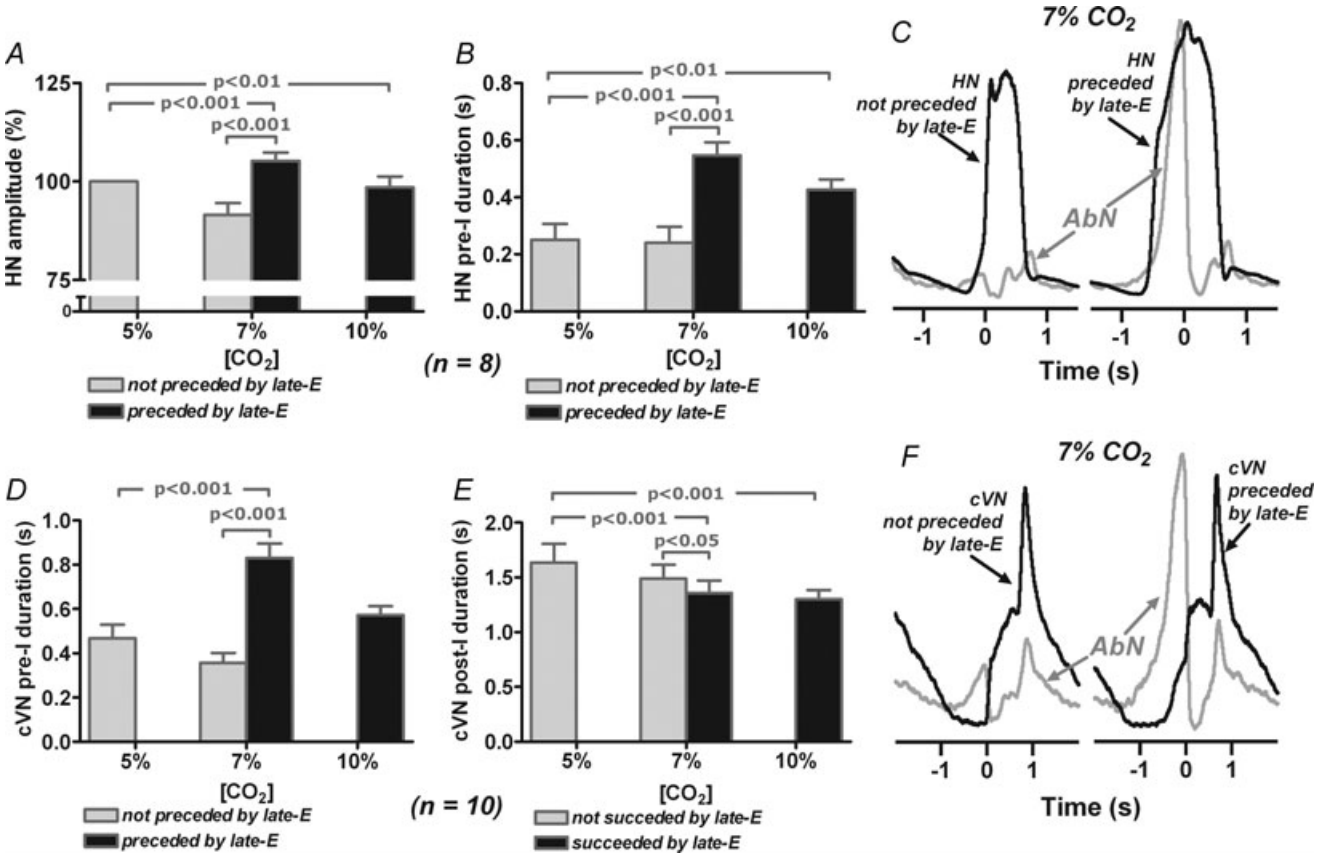

Figure 4. Occurrence of late-E abdominal (AbN) activity is correlated with alterations of cranial respiratory motor outflow patterns
At 7% CO_2, late-E AbN bursts were followed by increased amplitude (*A*) and advanced onset (*B*) of HN bursts. Black bars show cycles that were preceded by late-E AbN and grey bars, cycles that were not. *C*, representative CTAs show an average of 26 HN bursts (black) that were preceded by late-E AbN bursts (grey), and 24 cycles that were not. Time 0 marks onset of inspiration on PN. At 7% CO_2, late-E AbN bursts correlated with advanced onset (*D*) of following cVN burst and advanced offset of post-inspiratory (post-I) activities (*E*) of the preceding cVN bursts. *F*, representative CTAs were compiled from 20 cVN bursts (black) that were preceded by late-E AbN bursts (grey) and 30 that were not. All values represent mean ± S.E.M. (error bars).

hypercapnia up to 10%. The two-phase pattern persisted with sequential transections up to the rostral edge of BötC. A further transection to disconnect the BötC, one immediately rostral to the pre-BötC, abolished all expiratory activity in AbN, and released the one-phase pattern (Smith *et al.* 2007) consisting of synchronous inspiratory discharge in PN and cVN without AbN activity. We could not reinstate any AbN discharge by raising respiratory drive with the stimulants described above. These experiments indicate the importance of the pons for the expression of the late-E AbN activity. Whilst tonic AbN discharge persists after the pons is removed, this activity appears dependent on the BötC and/or RTN/vlPF since a transverse section at the rostral edge of the pre-BötC abolished all tonic expiratory activity. To assess the relative importance of the BötC *versus* the RTN/vlPF, we used discrete microinjection of a GABA receptor agonist (isoguvacine) to reversibly inactivate the RTN/vlPF region (see below).

Microinjection. In intact preparations generating the three-phase pattern, we approached the RTN/vlPF region

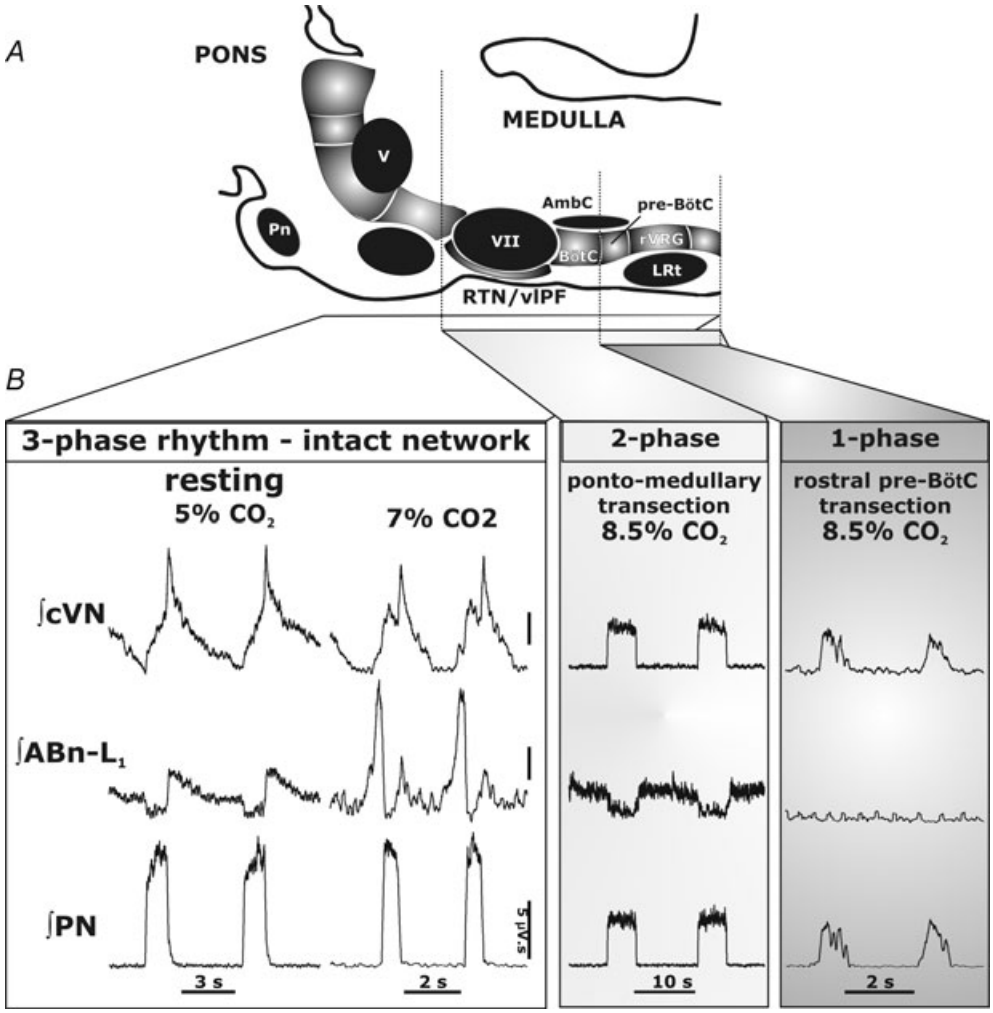

Figure 5
A, schematic diagram depicting the spatial arrangement of the ventral respiratory column viewed sagittally. We performed precise microtransections of the brainstem indicated by the vertical dashed lines (see Methods). *B*, activity patterns of phrenic (PN), spinal abdominal (AbN) and central vagus (cVN) nerves from an intact preparation (3-phase pattern) during eucapnia (5% CO_2) and hypercapnia (7% CO_2, $n = 15$), and after a ponto-medullary transection. This resulted in a 2-phase pattern in which late-E abdominal bursts are absent during hypercapnia (8.5% CO_2). AbN motor output displayed tonic activity throughout expiration, which decremented slightly in the late-E phase ($n = 8$). After a transection at the rostral boundary of the pre-BötC, a 1-phase pattern was evoked and all expiratory motor output was absent ($n = 8$). Abbreviations: AmbC: compact nucleus ambiguus; BötC: Bötzinger complex; LRt: lateral reticular nucleus; Pn: pontine nucleus; pre-BötC: pre- Bötzinger complex; RTN/vlPF: retrotrapezoid nucleus and ventrolateral parafacial regions; rVRG: rostral ventral respiratory group; V: trigeminal motor nucleus; VII: facial motor nucleus.

from the exposed ventral surface of the medulla and microinjected isoguvacine hydrochloride to reversibly hyperpolarize neurones in the RTN/vlPF region. Bilateral microinjections into the RTN/vlPF region induced a short transitory apnoea (< 30 s), inhibited post-I activity in both cVN and AbN outflows, with the PN exhibiting a 'square-wave' discharge shape with reduced amplitude ($35 \pm 7\,\mu$V *vs.* $22 \pm 6\,\mu$V, $P < 0.001$) and increased respiratory rate (from 24 ± 2 to 37 ± 4 breaths min^{-1}, $P < 0.001$, Fig. 6). In all cases, inactivation of the RTN/vlPF completely abolished hypercapnia-induced (10% CO_2) late-E bursting in both thoracic and lumbar AbN motor outflows (Fig. 6). In contrast, post-I activity in cVN recovered during hypercapnia, as well as the amplitude of PN discharge ($35 \pm 8\,\mu$V); this occurred probably due to the increased drive provided by the hypercapnia. The depressant effect of isoguvacine reversed after 1 h. Figure 7 shows a reconstructed topographical map of the microinjection sites made in the RTN/vlPF region. When microinjections were located in the RTN/vlPF at the level of the caudal half of the facial nucleus and aligned laterally with nucleus ambiguus, the most potent inhibition of AbN motor outflow (both post-I and late-E) was obtained. Microinjections that were too deep below the RTN/vlPF (i.e. entering into the facial motor nucleus) or that were superficial but lateral to nucleus ambiguus, or rostral to the midpoint of the facial nucleus or caudal to its caudal edge, had little or no effect on late-E AbN activity and the ongoing respiratory rhythm.

These results indicate that activity of RTN/vlPF appears important for the expression of late-E AbN activity induced by hypercapnia. Regarding the underlying mechanisms, we considered two possibilities: either the RTN/vlPF provides excitatory drive into the BötC, which is responsible for the generation of late-E AbN activity, or the RTN/vlPF region contains late-E expiratory neurones itself.

Inactivation of RTN/vlPF region: effect on BötC augmenting expiratory activity

We performed population neurone recordings from the BötC using tungsten electrodes while simultaneously inactivating the RTN/vlPF bilaterally by microinjecting isoguvacine ($n = 6$). Initially, single unit recordings were attempted but could not be stably maintained during the microinjection. After suppression of the RTN/vlPF by isoguvacine, late-E AbN activity (induced by hypercapnia, 7% CO_2) was abolished but ongoing aug-E population activity in the BötC persisted (Fig. 8*A*). Figure 8*B* shows PN CTAs of BötC aug-E neurones under hypercapnia (7% CO_2), only in those cycles when late-E AbN activity did not occur (skipping). Figure 8*C* shows that the occurrence of late-E AbN bursts was tightly correlated with an

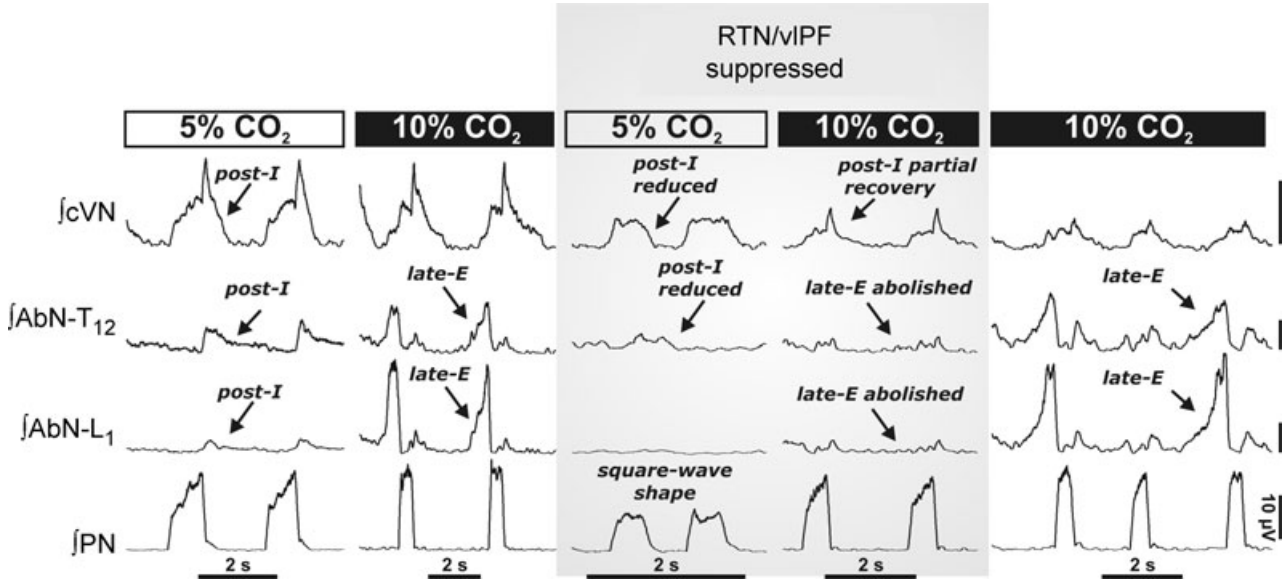

Figure 6. The retrotrapezoid/ventrolateral parafacial regions (RTN/vlPF) are relevant for the 3-phase respiratory rhythm and generation of late-E abdominal (AbN) activity
Hypercapnia (10% CO_2) induces late-E bursts in the AbN (T_{12}–L_1) (left). Bilateral microinjections ($n = 11$) of isoguvacine hydrochloride ($GABA_A$ receptor agonist) to suppress the RTN/vlPF region disrupted the 3-phase respiratory rhythm during eucapnia (5% CO_2). Post-inspiratory motor output on both AbN and central vagus (cVN) nerves was reduced and phrenic nerve pattern (PN) was transformed to a 'square-wave' shape. RTN/vlPF suppression also abolished late-E AbN bursts during hypercapnia (10% CO_2). Late-E activity recovered after isoguvacine was washed out (~1 h) (right panel). All traces show integrated nerve activities.

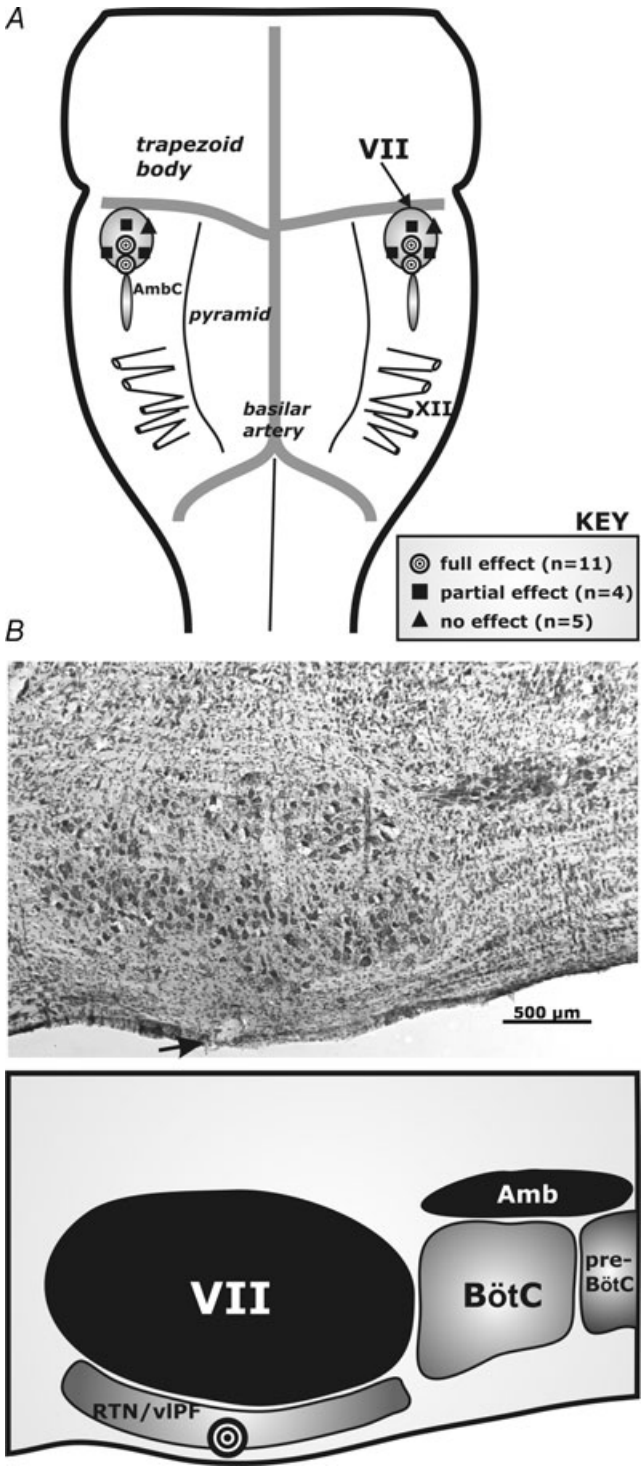

Figure 7
A, we microinjected dye (Pontamine sky blue) after experiments to allow a topographical mapping of the microinjection sites into the retrotrapezoid/ventrolateral parafacial regions (RTN/vlPF). Microinjection centres located in the caudal half of the facial nucleus (VII) and aligned at the medial lateral level of the compact division of nucleus ambiguous (AmbC) produced the most potent inhibition of expiratory motor outflow (both post-I and late-E). *B*, example of a sagittal section (40 μm, neutral red) of a brainstem at the level of facial nucleus (VII) and the Bötzinger complex (BötC) with a stained microinjection site (arrow); the schematic diagram depicts the outline of the relevant respiratory-related regions. Other abbreviations: Amb: nucleus ambiguus; pre-BötC: pre-Bötzinger complex; XII: hypoglossal nerve rootlets.

increase in maximum firing frequency of BötC activity that occurred coincident with the late-E AbN discharge (see also Fig. 8*E*). The suppression of RTN/vlPF abolished both the late-E AbN bursting and the BötC late-E firing coupled with it. However, the basal BötC augmenting-E activity did not differ significantly from control after RTN/vlPF inhibition (Fig. 8*D* and *E*). The microinjections of isoguvacine in these experiments were confined to the regions that most effectively abolished late-E AbN discharge and coincided with those described above (see Fig. 7).

Is there rhythmic late-E expiratory activity in the RTN/vlPF region?

In order to test for the existence of rhythmic late-E expiratory activity in the RTN/vlPF region, we recorded single neurone activity (tungsten steel, 10 M; and 3 M NaCl-filled glass microelectrodes, 15–20 M). In the presence of hypercapnia (7% CO_2), we found tonically firing units that were CO_2 sensitive and responded to peripheral chemoreceptor activation (Fig. 9*B*, $n = 5$) as reported by others (Fortuna *et al.* 2008). However, we also found rhythmically active units that only fired coincidently with AbN late-E discharge in hypercapnia (7% CO_2; $n = 7$ cells from 5 preparations; Fig. 9*A*). Interestingly, when late-E AbN activity skipped a respiratory cycle, these units were also silent for this cycle. Compared to the augmenting BötC neurons, the onset of firing of the RTN/vlPF cells was always later but coincided with the onset of the late-E AbN discharge. Switching from hypercapnia to eucapnia (5% CO_2) allowed us to study the transitional slow disappearance of late-E AbN bursts. This was seen as intermittent late-E AbN firing which became less frequent until it ceased. In all cases ($n = 7$), RTN/vlPF expiratory neurone firing only occurred when the late-E AbN discharged. In eucapnia, when late-E AbN activity was abolished, these neurones were silent in all cases but were re-activated on reinstating hypercapnia. The RTN/vlPF units were located superficially (i.e. $< 100\,\mu$m beneath the ventral surface of the medulla) and were located $\sim$0.5 mm caudal to the caudal end of the trapezoid body (within the caudal half of the facial nucleus), which corresponded to the sites at which neuronal inactivation blocked AbN motor activity in hypercapnia.

Discussion

The present study has extended our current knowledge of the central control of abdominal expiratory activity in the rat. During eupnoea the AbN motor discharge exhibited a low-amplitude post-I discharge only. Switching to various hypoxic/hypercapnic conditions (hypercapnic hypoxia, eucapnic hypoxia and peripheral chemoreceptor activation) evoked well-expressed biphasic-E discharges in the AbN, which were identical (especially in neonates) to those described previously by others (Janczewski *et al.* 2002; Janczewski & Feldman, 2006*a*; Onimaru *et al.* 2006; Taccola *et al.* 2007). Normoxic hypercapnia, however, evoked high-amplitude late-E bursting in the AbN outflow comparable to that seen *in vivo* in decerebrate rats (Iizuka & Fregosi, 2007). In our preparation, 7% CO_2 induced increases in respiratory frequency only in respiratory cycles that did not express late-E AbN bursts, whereas cycles containing late-E bursts showed a small decrease in frequency compared to eucapnia. It would appear that the excitatory effects on expiratory activity (late-E) are sufficient to prolong the expiratory interval causing a mild slowing of frequency at least in our experimental conditions when lung inflation feedback is absent. There is evidence that intact vagal feedback from lungs is essential for tachypnoea in response to hypercapnia. (Phillipson, 1974; Harris & Milsom, 2001).

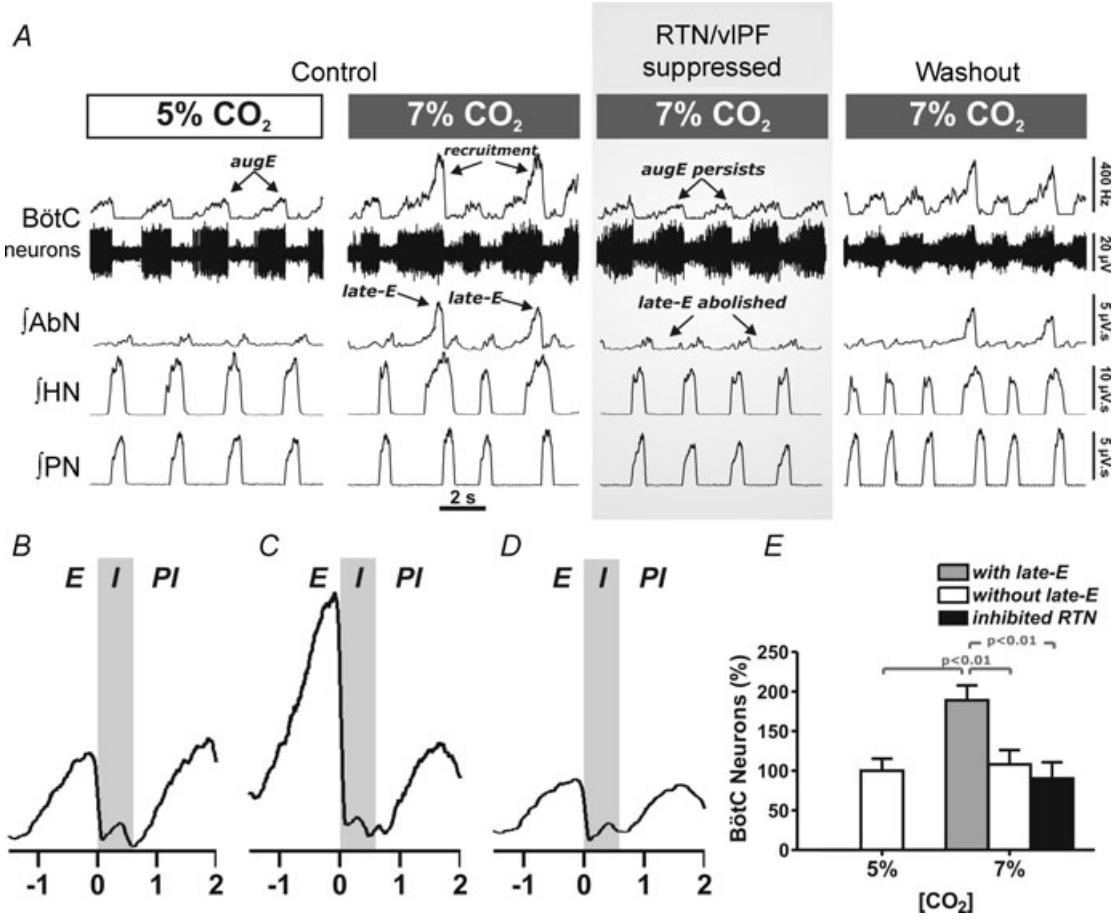

Figure 8. Suppression of RTN/vlPF does not affect BötC augmenting E activity but abolishes late-E abdominal discharge

To assess the relevance of the Bötzinger complex (BötC) for late-E abdominal activity, we recorded augmenting expiratory (aug-E) population activity in the BötC simultaneously with phrenic (PN), abdominal (AbN) and central vagus (cVN) nerves as we inhibited the RTN/vlPF region (*A*). Bilateral microinjections of a $GABA_A$ agonist into the RTN/vlPF region abolished AbN late-E bursts completely, but central aug-E activity persisted in the BötC. CTA of integrated BötC population activities under 7% CO_2 in cycles that do not contain late-E AbN bursts (*B*), containing late-E bursts (*C*) and after RTN/vlPF was suppressed (*D*). Time 0 indicates beginning of PN inspiration and grey area indicates duration of inspiration. *E*, maximum firing frequency (% of control at 5% CO_2) of BötC augmenting E population before and after RTN/vlPF inhibition. Note that maximum firing frequency of BötC population was increased in association with late-E AbN bursts, and both were abolished by RTN/vlPF suppression, but baseline BötC activity persisted.

After ponto-medullary transection that spared the RTN/vlPF region, the three-phase pattern of respiratory activity (inspiration, post-inspiration and expiration) transformed into a two-phase pattern lacking post-I activity in the central vagus motor outflow (as in Smith *et al.* 2007) accompanied by weak expiratory motor activity in the AbN that was silenced during inspiration (phrenic activity). Subsequent hypercapnia never reinstated the late-E bursts. In brainstem-intact preparations that were made hypercapnic, inactivation of the RTN/vlPF region abolished both AbN and BötC late-E bursting despite most of the regular BötC aug-E activity remaining. We identified rhythmically active late-E neurones in the RTN/vlPF region whose firing was coincident to late-E AbN bursting in hypercapnia but these neurones were quiescent in eupnoea.

The results of our study provided a number of new insights into the control of expiration. (1) First abdominal nerve recordings from the *in situ* rat preparation. We believe this is important as this preparation is used by many researchers in respiratory control. (2) Comparative analysis of abdominal nerve activity from different segmental levels. (3) First presentation of abdominal nerve activity with three other respiratory motor outflows recorded simultaneously and their comparison in neonatal *versus* juvenile rats during different metabolic conditions.

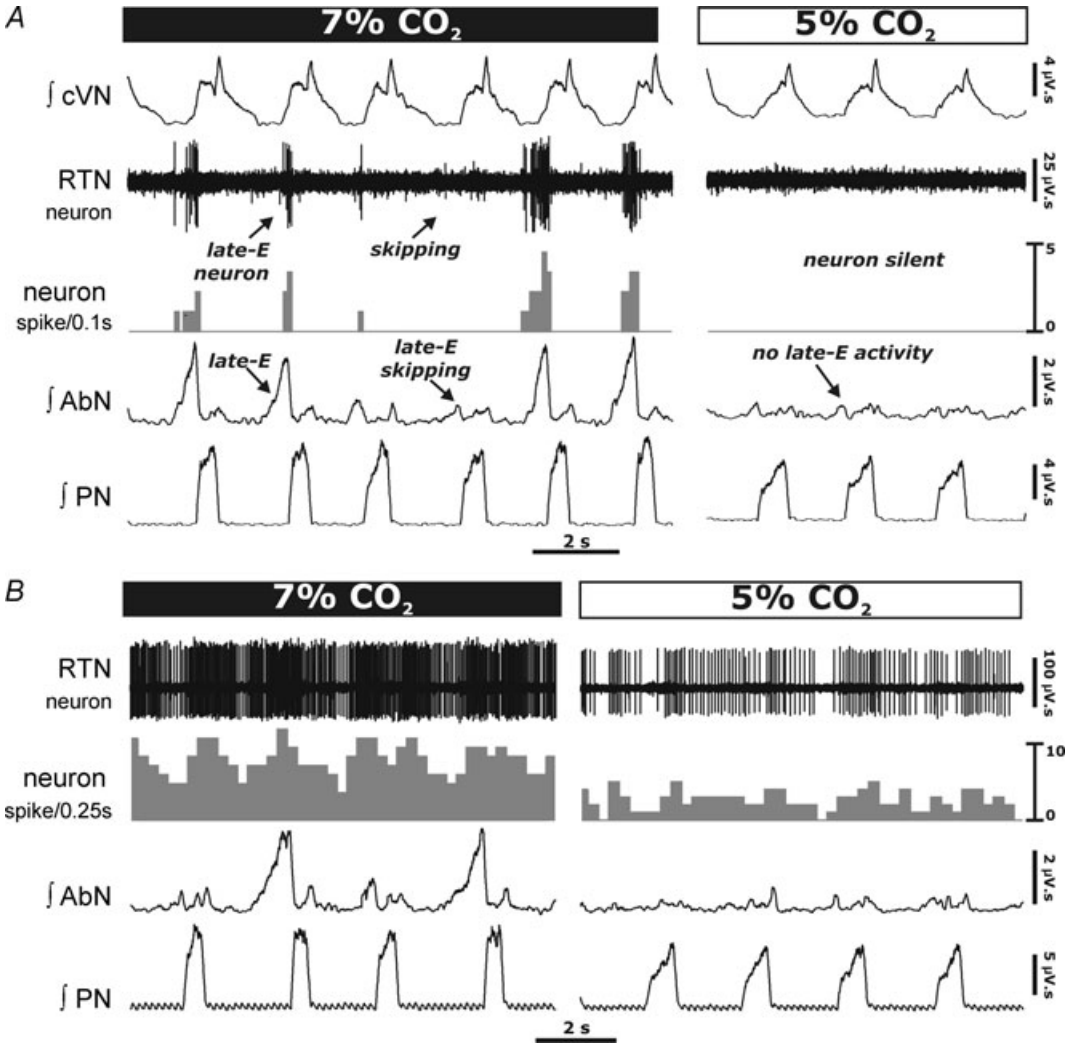

Figure 9. Examples of two types of neurones recorded in the same region of the RTN/vlPF during hypercapnia

Traces show integrated phrenic (PN), spinal abdominal (AbN), central vagus (cVN) nerve activities and neurone recorded in RTN/vlPF region with firing rate histograms. *A*, an example of a rhythmically active late-E neuron. Under hypercapnia (7% CO_2), these cells ($n = 7$ from 5 juvenile rats) fired exclusively in phase with late-E abdominal bursts, but were quiescent in the absence of late-E AbN bursts as in eucapnia (5% CO_2). *B*, example of a RTN CO_2-sensitive tonic neurone reported previously (Fortuna *et al.* 2008) which was intermingled with the neurone in *A*.

(4) Identification of post-inspiratory activity in the abdominal nerve of rats. (5) A phase analysis with central vagal motor outflow allowing an assessment of the influence of abdominal nerve activity on post-inspiration. (6) A phase analysis with hypoglossal motor activity revealing insights into a relationship with pre-inspiratory activity and upper airway control.

Our results have helped clarify a series of important issues raised in the Introduction. The discussion below focuses on these questions.

Is there a separate 'oscillator' that drives AbN late-E motor activity during forced expiration and, if so, where is it located?

We observed that the expression of AbN expiratory activity (post-I and late-E) requires the presence of both the pons and RTN/vlPF. Previously, we showed that the pons was essential for post-I activity recorded from the cVN and BötC and for the generation of the eupnoeic three-phase respiratory pattern (Smith *et al.* 2007). Moreover, we found that both the pons and the RTN/vlPF are essential for expression of late-E AbN bursting induced by hypercapnia, which may have a bearing on where late-E activity is generated. Based on our data, it is very possible that the pons provides tonic excitatory drive to a neural population located within the ventral respiratory column that is necessary for generation of late-E activity. Our data, however, do not allow a definite conclusion to whether this activity is generated within or relayed through the RTN/vlPF region. There is evidence that the pons mediates the reduction in expiratory time during hypercapnia (Song & Poon, 2009). Janczekski & Feldman (2006*a*,*b*) have proposed that the RTN/vlPF is a site for the generation of biphasic-E activity. We found that inactivation of RTN/vlPF in hypercapnia abolished late-E activity in both the BötC and AbN, and late-E neurones in RTN/vlPF firing coincidently with AbN late-E bursts. This only shows that this region is essential for the expression of late-E AbN bursting but does not necessarily imply that it is a rhythmogenic site for late-E activity.

It is known that some RTN/vlPF neurones project to the retroambiguual region, the site of pre-motor bulbospinal expiratory neurones (Fortuna *et al.* 2008). This provides an explanation for our observation that inactivating the RTN/vlPF abolished AbN motor activity but failed to arrest ongoing aug-E activity in BötC. This is also consistent with the paucity of BötC neurones projecting to pre-motor abdominal motoneurones (Iscoe, 1998; Fortuna *et al.* 2008). Although low *versus* high threshold motoneurons may be recruited with increased respiratory drive, we propose that distinct neural populations generate late-E and aug-E activities. First, RTN/vlPF inactivation depresses late-E but not BötC aug-E activity; second, during sneezing, in the cat, aug-E neurones in BötC are quiescent yet the abdominal muscles contract (Orem & Brooks, 1986). Therefore, we suggest that late-E neurones in the RTN/vlPF neurones are distinct from BötC neurons and that both populations may be recruited under conditions of enhanced expiratory demand to accelerate expiration. We conclude that high respiratory drive activates a distinct late-E generator and that the RTN/vlPF plays a critical role in the expression of late-E activity in AbN, and is either the late-E generator or a relay. An alternate source of late-E activity may be in the pons. Although unknown, the rhythmogenic circuits involved in generation of AbN late-E activity under hypercapnia/hypoxia may represent a fourth oscillatory mechanism in addition to the three others described previously (Smith *et al.* 2007).

Is this expiratory 'oscillator' a necessary component of the respiratory central pattern generator (CPG), and does it operate under eupnoeic conditions?

Onimaru *et al.* (1987, 1988, 2006) have suggested that '*pre-inspiratory*' neurones constitute the primary *inspiratory* oscillator that promotes the activity of the 'secondary' inspiratory oscillator in the pre-BötC. The so called '*pre-inspiratory*' activity found originally *in vitro* by Onimaru *et al.* (1987) is characterized as having a burst discharge prior to, and immediately after, PN (spinal C_4) activity and termed here as biphasic-E. This biphasic-E activity was recorded from, and presumed to be generated within, the pFRG of *en bloc in vitro* brainstem preparations of neonatal rats (Onimaru *et al.* 1987, 1988, 2006). Onimaru *et al.*'s concept would require these cells to express an excitatory phenotype and to be rhythmically active in juvenile animals under normal eupnoeic conditions; however, many failed to demonstrate this *in vivo* (Connelly *et al.* 1990; Fortuna *et al.* 2008). Instead, in the anaesthetized *in vivo* adult rat, Fortuna *et al.* (2008) found neurones displaying a biphasic-E pattern but these neurones were located only in the BötC despite surveying the RTN/vlPF. Incidentally, biphasic-E neuronal activity appears to diminish after the first postnatal day of life (see Oku *et al.* 2007) suggesting either a migration of these neurones or loss of such activity as the network develops. A failure to find biphasic-E neurones may also be explained by inadequate exploring of the region. Our recording sites were based on effective microinjection sites which only partially overlap with the pFRG (Onimaru & Homma, 2003). Additionally, Fortuna *et al.* (2008) found that only severe hypoxic hypercapnia could induce the hallmark biphasic-E pattern, suggesting that this activity was highly state dependent. The biphasic-E neurones found by Fortuna *et al.* (2008) in the BötC were glycinergic, which is contrary to the suggested excitatory

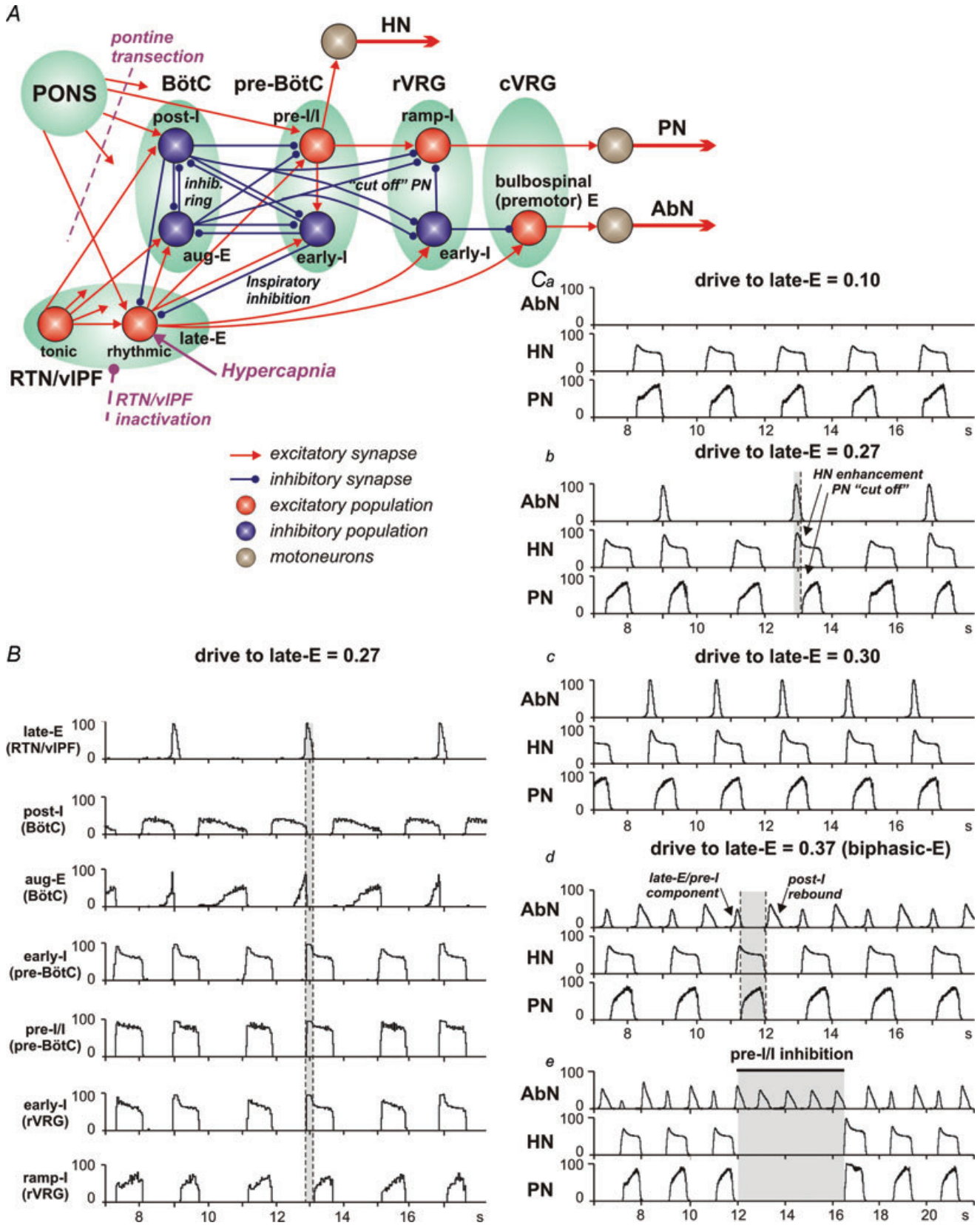

Figure 10. Extended model of the brainstem respiratory network
(See detailed description in Smith *et al.* 2007.) *A*, schematic diagram of the extended model showing interactions between specific populations of respiratory neurones within major brainstem respiratory compartments

role of biphasic-E neurones proposed by Onimaru *et al.* (2006). Finally, developmental differences cannot explain the differences between neonatal *in vitro* studies and juvenile animals. Our neonatal *in situ* rats showed identical AbN outflows to juveniles under conditions of both eupnoea and high respiratory drive.

Janczewski & Feldman (2006*b*) working with anaesthetized, *in vivo*, pontine intact and pontine transected neonatal rats have suggested that this same biphasic-E activity represents a separate and independent '*expiratory oscillator*' located within the RTN/vlPF that couples with the pre-BötC inspiratory oscillator providing a fundamental mechanism for respiratory rhythm generation. It follows that these oscillators may have reciprocal inhibitory interactions. However, whilst biphasic expiratory neurones described by Fortuna *et al.* (2008) were inhibitory, they were localized to the BötC, not RTN/vlPF, and were only active under hypercapnia and hypoxia. It has also been suggested (Feldman & Del Negro, 2006; Janczewski & Feldman, 2006*a*,*b*) that this RTN/vlPF oscillator is intrinsically rhythmic but neuronal recordings to test this have not been performed. Moreover, the RTN/vlPF–pre-BötC as a unit generating the eupnoeic rhythm is disputed, as biphasic-E activity was not found in the RTN/vlPF region of juvenile animals exhibiting normal breathing or under hypercapnia (this study; Fortuna *et al.* 2008). We suggest that the *in vivo* pontine-transected anaesthetized rat preparation (Janczewski & Feldman, 2006*a*) was in a state of high respiratory drive (perhaps caused by haemorrhage) resulting in forced expiration, a possibility that has been previously acknowledged (e.g. Feldman & Del Negro, 2006). Our current and previous studies indicate that removal or inactivation of the RTN/vlPF, while abolishing AbN late-E activity, does not stop the ongoing BötC expiratory activity. Hence, the remaining BötC and pre-BötC network interactions provide a two-phase pattern of activity independent of the RTN/vlPF as suggested previously (Shen *et al.* 2003; Smith *et al.* 2007).

Why Fortuna *et al.* (2008) were unable to locate late-E firing neurones in the RTN is unknown, but we suggest possible reasons. First, unlike Fortuna *et al.* (2008), we searched for late-E neurones in hypercapnia not eucapnia, a state in which they were silent and may therefore have been missed. We recorded in the same region as Fortuna *et al.* (2008) based on the anatomical location. We found intermingled with the late-E neurones, CO_2-sensitive tonically firing neurones like those described by Guyenet *et al.* (2005). Second, we used a decerebrate unanaesthetized rat model compared to a brain-intact anaesthetized rat to avoid any possible depressant actions of anaesthesia. Third, we directly recorded AbN activity which is especially relevant since the late-E cells we recorded skipped respiratory cycles at 7% CO_2. Clearly, additional experiments are needed to further assess the spatial distribution and determine the neurochemical content and biophysical properties of the type of late-E neurones we recorded in the RTN/vlPF region. A final consideration is that interactions between the late-E (pre-I) neurons of RTN/vlPF and pre-Bötzinger inspiratory neurons may vary with postnatal age (Wittmeier *et al.* 2008).

In summary, our answer to the second question posed above is: no, the ultimate 'expiratory oscillator' does not operate during normal eupnoeic breathing in the rat, as hypothesized (Iscoe, 1998; Feldman & Del Negro, 2006), but is only activated under conditions of high central respiratory drive. Since the eupnoeic respiratory rhythm is generated without activation or involvement of this 'expiratory oscillator', the latter cannot be considered a necessary or fundamental component of the respiratory central pattern generator. Of course, we cannot rule

(pons, RTN/vlPF, BötC, pre-BötC, rVRG and cVRG). Each population (shown as a sphere) consists of 50 neurons described in the Hodgkin–Huxley style. This model incorporates an additional late-E population in the RTN/vlPF. This population is identical to the pre-I/I population in the pre-BötC and consists of 50 neurones containing persistent sodium current and interconnected with mutually excitatory connections (Smith *et al*. 2007). Most connections are based on previously published experimental data (for references see Smith *et al.* 2007) and some are suggested (*ibid*). The model includes proposed interactions between the late-E neuronal population in the RTN/vlPF, activated by hypercapnia, and other populations of respiratory neurones. Interactions between late-E and pre-I/I populations are similar to those proposed by Wittmeier *et al.* (2008). *B* and *Ca–e* show activity of selected neuronal populations in the model (*B*) and motor outputs (AbN, HN, PN in *Ca–e*). Activity of each population is represented by a histogram of average neuronal spiking frequency within the population (spikes s^{-1} $neurone^{-1}$, bin size 30 ms). Hypercapnia was simulated by an additional 'hypercapnia-evoked' drive to the late-E population of RTN/vlPF. In *B* and *Cb*, the value of this drive was 0.27 (arbitrary units). In *Ca–d/e*, this drive progressively increased (indicated above each diagram). The late-E activity was expressed and increased frequency with the increase of this drive (*Ca–c*). Increasing drive above 0.35 converted the late-E pattern in the late-E population and AbN output to biphasic-E, containing a rebound post-I component (*Cd*, see also Wittmeier *et al.* 2008). Also similar to the Wittmeier *et al.* model, suppression of the pre-I/I population in the pre-BötC (by direct inhibition) to simulate the effects of opioids (Janczewski & Feldman, 2006*a*) eliminates inspiratory inhibition of the late-E population by the early-I population of pre-BötC, and converts the biphasic-E bursts in AbN to prolonged monophasic discharges lacking the rebound post-I component (*Ce*).

out that neuronal late-E activity may exist even in the absence of AbN motor output. However, because the late-E neurones may excite the pre-BötC pre-I/I neurones (see below) to promote the onset of inspiration (Onimaru *et al.* 1987, 1988, 2006) and also drive pre-motor circuits that generate AbN expiratory activity (Feldman & Del Negro, 2006; Janczewski & Feldman, 2006*a,b*; this study), this oscillator may not represent an 'expiratory' oscillator *per se*. Rather it is activated under critical metabolic conditions (hypercapnia, hypoxia) to coordinate/entrain both inspiration and active expiration (see below).

How does late-E expiratory activity influence the brainstem respiratory network?

We have extended our previously published computational model of the respiratory CPG (Smith *et al.* 2007) by incorporating an additional late-E population in the RTN/vlPF (Fig. 10). This population consisted of 50 neurones containing persistent sodium current (I_{NaP}) and interconnected with mutually excitatory connections. PN and HN motoneurones in this model received independent drives (Peever *et al.* 2001). Interactions between the pre-BötC and RTN/vlPF were similar to the minimal model of Wittmeier *et al.* (2008). In our model, the late-E population provides excitation to the pre-BötC pre-I/I and early I populations. In turn, the inhibitory early-I population (Fig. 10*A*) inhibits the late-E. We have also proposed that the late-E population receives a necessary drive from the pons, which under eupnoeic breathing conditions is not sufficient to evoke rhythmic activity (see Fig. 10*Ca*). We suggest that hypercapnia provides an additional excitatory drive to late-E neurones that potentially can switch on their bursting state (see Fig. 10*A*). By the end of expiration the post-I population reduce their inhibition over late-E allowing the bursts to emerge (Fig. 10*B* and *Cb*). When this happens, each late-E burst excites the pre-I/I population producing earlier onset of pre-I activity. Then, the early-I population of the pre-BötC inhibits the late-E (Fig. 10*A* and *B*), hence the short-duration, high-amplitude late-E bursts observed (Fig. 10*B*, see also Wittmeier *et al.* 2008). We suggest that the late-E bursts in the RTN/vlPF excite abdominal motoneurones either directly, or via pre-motor bulbospinal BötC neurones, or via the pre-motor bulbospinal neurones located in cVRG (Fig. 10*A*, *Cb* and *c*). Because the late-E bursts excite the pre-I/I population in the pre-BötC they also contribute to the earlier onset and enhancement of the pre-I component of HN discharge (see Figs 2*A* and *B* and 4*C*, and Fig. 10*B* and *Cb–d*). We accept that the HN discharge in our model has a somewhat different profile to the experimental records. In addition, the late-E neurones excite the aug-E cells in the BötC and the early-I cells of rVRG (Fig. 10*A*, Fig. 8*A*), which inhibit the rVRG ramp-I premotor neurons, thereby 'cutting off' the initial part of PN ramp (see Figs 2*A* and *B*, 3*F*, and Fig. 10*B* and *Cb–d*). This may explain the shortening of PN burst duration (Fig. 3*B*) without significant change in period and amplitude.

With progressive increases of hypercapnia-evoked drive to the late-E population, the late-E burst emerges more frequently (Fig. 10*Cc*). This simulated behaviour is fully consistent with our experimental data (Fig. 2) and that of Iizuka & Fregosi (2007, see Fig. 2 in that paper). A further increase of this drive produces biphasic-E bursts consisting of a late-E/pre-I component and post-I rebound in AbN (Fig. 10*Cd* and *e*; see also Wittmeier *et al.* 2008). As in the Wittmeier *et al.* (2008) model, suppression of the pre-I/I population in the pre-BötC in our model simulates the effects of opioids (Janczewski & Feldman (2006*a*), and eliminates inspiratory inhibition of late-E, which converts the biphasic-E bursts in AbN to prolonged monophasic discharges lacking the rebound component (Fig. 10*Ce*). The biphasic-E pattern in the late-E population and AbN output (Fig. 10*Cd* and *Ce*) has not been observed during normoxic hypercapnia (our data) or hyperoxic hypercapnia (Iizuka & Fregosi, 2007). We suggest that an additional drive from peripheral chemoreceptors (i.e. hypoxic hypercapnia) is necessary to evoke such biphasic-E activity.

Our previous modelling studies (Rybak *et al.* 2007; Smith *et al.* 2007) predicted that both the pons and RTN provide excitatory drive to post-I population in the BötC. Both of these drives are essential for the generation of the eupnoeic three-phase respiratory rhythm. In the current model, we suggest that the late-E population of RTN/vlPF receives a necessary drive from the pons. Therefore, removal of the pons or suppression of the RTN/vlPF (Fig. 10*A*) could maintain the expressed AbN expiratory activity but would abolish the late-E discharges in the AbN. Note, however, that our current model only considers one possible scenario, that being when late-E activity originates in RTN/vlPF. We cannot rule out (and have not modelled) another possibility that late-E activity is generated in the pons by some late-E and aug-E neurones projecting to the VRC (see Ezure & Tanaka, 2006; Song *et al.* 2006; Wittmeier *et al.* 2008). Further, RTN chemoreceptors could provide a necessary drive to these pontine neurones. Both the latter mechanisms would fail after pontine transection to abolish late-E abdominal activity.

What is the functional relevance of late-E activity?

Under eucapnia, we observed that lower thoracic AbN exhibited a higher amplitude post-I burst compared to the upper lumbar levels. Under hypercapnia, the converse was true for late-E bursts, which exhibited significantly higher amplitudes at the lumbar level. *In vivo*, under normal conditions, expiration is passive and

low amplitude abdominal post-I activity in the vicinity of the diaphragm (i.e. thoracic level especially) would increase muscle tone in the upper abdomen. We suggest that this would provide stable anchoring during recoil of the diaphragm to allow controlled release of expired air. Late-E abdominal activity functionally constitutes forced expiration, which only occurs in certain conditions such as asphyxia and moderate/intense exercise. We observed that the late-E activity is recruited more strongly in lumbar abdominal nerves. Interestingly, abdominal late-E bursts were correlated with a substantial increase of pre-I activity in the cranial motor outflows (Fig. 2). This would serve to advance the reduction in upper airway resistance thereby timing it with forced expiration. Thus, pre-I activity in cranial motor outflows could serve to reduce airflow resistance to expired air timed with abdominal forcing. This reduction in resistance continues into the inspiratory phase of the subsequent breath. Thus, under conditions of forced breathing an ingenious common mechanism is in place to assist airflow in both the expiratory and inspiratory directions during late-E and inspiration, respectively.

A previous study in the decerebrate, vagotomized cat showed abolition of abdominal discharge during gasping (St-John *et al.* 1989). Herein, gasping was associated with a biphasic-E discharge in juveniles and neonates, which was similar to that seen in a brainstem spinal cord *in vitro* preparation from neonatal rat made anoxic (Taccola *et al.* 2007). Whether this reflects a species difference is unclear. Alternately, late-E abdominal activity decreases lung volume below functional residual capacity so that inspiratory volume would be maximal. However, the rat has a functional residual capacity of only 25% of total lung volume, which limits the physiological relevance of forced end-expiration in this species (Fisher & Mortola, 1980). At the end of the phrenic burst, post-I (abdominal) would aid complete emptying of the lungs.

The pattern of abdominal motor activity we report in hypercapnia (recruitment of late-E activity) is consistent with that reported previously in EMG recordings from rectus abdominis *in vivo* from both rat (Sherrey *et al.* 1988) and man (Strohl *et al.* 1981; Oliven *et al.* 1985) subjected to high respiratory drive conditions (see review by Iscoe, 1998). In contrast, no abdominal EMG activity was discernible in sleeping rat (non-rapid eye movement; Sherrey *et al.* 1988) and supine man (Strohl *et al.* 1981) under eucapnic conditions, unlike in this report where a low amplitude post-I discharge was recorded in AbN. Possible reasons for this difference are as follows. (1) Due to the very low amplitude, this activity may be subthreshold and is unlikely to be detectable in EMG recordings. (2) We were better placed to discriminate this motor nerve activity from nearby post-I activity of the diaphragm (see Sherrey *et al.* 1988). (3) The abdominal motor outflow of a quadruped may be distinct to a biped and the posture at the time of recording may also affect when this activity is expressed.

Finally, recent studies have demonstrated that late-E abdominal activity is present during eupnoea in the perfused preparation of rats submitted to chronic intermittent hypoxia (CIH, Zoccal *et al.* 2008). Under these conditions late-E AbN activity was phase-correlated with an additional burst of sympathetic activity. Further, Simms *et al.* (2009) demonstrated a causal correlation for enhanced respiratory modulation of sympathetic activity and increase in vascular resistance. Based on this, we propose that the chronic expression of late-E AbN activity may contribute to the hypertensive states in both SHR and CIH rat models and therefore, can be pathological.

References

Abraham KA, Feingold H, Fuller DD, Jenkins M, Mateika JH & Fregosi RF (2002). Respiratory-related activation of human abdominal muscles during exercise. *J Physiol* **541**, 653–663.

Ballanyi K, Onimaru H & Homma I (1999). Respiratory network function in the isolated brainstem–spinal cord of newborn rats. *Prog Neurobiol* **59**, 583–634.

Ballanyi K, Volker A & Richter DW (1994). Anoxia induced functional inactivation of neonatal respiratory neurones in vitro. *Neuroreport* **6**, 165–168.

Cohen MI (1979). Neurogenesis of respiratory rhythm in the mammal. *Physiol Rev* **59**, 1105–1173.

Connelly CA, Ellenberger HH & Feldman JL (1990). Respiratory activity in retrotrapezoid nucleus in cat. *Am J Physiol Lung Cell Mol Physiol* **258**, L33–L44.

Ezure K (1990). Synaptic connections between medullary respiratory neurons and considerations on the genesis of respiratory rhythm. *Prog Neurobiol* **35**, 429–450.

Ezure K & Tanaka I (2006). Distribution and medullary projection of respiratory neurons in the dorsolateral pons of the rat. *Neuroscience* **141**, 1011–1023.

Ezure K, Tanaka I & Kondo M (2003). Glycine is used as a transmitter by decrementing expiratory neurons of the ventrolateral medulla in the rat. *J Neurosci* **23**, 8941–8948.

Feldman JL & Del Negro CA (2006). Looking for inspiration: new perspectives on respiratory rhythm. *Nat Rev Neurosci* **7**, 232–242.

Fisher JT & Mortola JP (1980). Statics of the respiratory system in newborn mammals. *Respir Physiol* **41**, 155–172.

Fortuna MG, West GH, Stornetta RL & Guyenet PG (2008). Bötzinger expiratory-augmenting neurons and the parafacial respiratory group. *J Neurosci* **28**, 2506–2515.

Fregosi R (1994). Influence of hypoxia and carotid sinus nerve stimulation on abdominal muscle activities in the cat. *J Appl Physiol* **76**, 602–609.

Fregosi R & Bartlett D Jr (1988). Central inspiratory influence on abdominal expiratory nerve activity. *J Appl Physiol* **65**, 1647–1654.

Guyenet PG, Mulkey DK, Stornetta RL & Balyliss DA (2005). Regulation of ventral surface chemoreceptors by the central respiratory pattern generator. *J Neurosci* **25**, 8938–8947.

Harris MB & Milsom WK (2001). Vagal feedback is essential for breathing in unanesthetized ground squirrels. *Respir Physiol* **125**, 199–212.

Iizuka M (2003). $GABA_A$ and glycine receptors in regulation of intercostal and abdominal expiratory activity *in vitro* in neonatal rat. *J Physiol* **551**, 617–633.

Iizuka M & Fregosi R (2007). Influence of hypercapnic acidosis and hypoxia on abdominal expiratory nerve activity in the rat. *Resp Physiol Neurobiol* **157**, 196–205.

Iscoe S (1998). Control of abdominal muscles. *Prog Neurobiol* **56**, 433–506.

Janczewski WA & Feldman JL (2006*a*). Distinct rhythm generators for inspiration and expiration in the juvenile rat. *J Physiol* **570**, 407–420.

Janczewski WA & Feldman JL (2006*b*). Novel data supporting the two respiratory rhythm oscillator hypothesis. Focus on 'respiration-related rhythmic activity in the rostral medulla of newborn rats'. *J Neurophysiol* **96**, 1–2.

Janczewski WA, Onimaru H, Homma I & Feldman JL (2002). Opioid-resistant respiratory pathway from the preinspiratory neurones to abdominal muscles: *in vivo* and *in vitro* study in the newborn rat. *J Physiol* **545**, 1017–1026.

Jiang C & Lipski J (1990). Extensive monosynaptic inhibition of ventral respiratory group neurons by augmenting neurons in the Bötzinger complex in the cat. *Exp Brain Res* **81**, 639–648.

Oku Y, Masumiya H & Okada Y (2007). Postnatal developmental changes in activation profiles of the respiratory neuronal network in the rat ventral medulla. *J Physiol* **585**, 175–186.

Oliven A, Kelsen SG, Deal EC Jr & Cherniack NS (1985). Respiratory pressure sensation. Relationship to changes in breathing pattern and PCO2 during acute increase in airway resistance in patients with chronic obstructive pulmonary disease. *Am Rev Respir Dis* **132**, 1214–1218.

Onimaru H, Arata A & Homma I (1987). Localization of respiratory rhythm-generating neurons in the medulla of brainstem–spinal cord preparations from newborn rats. *Neurosci Lett* **78**, 151–155.

Onimaru H, Arata A & Homma I (1988). Primary respiratory rhythm generator in the medulla of brainstem–spinal cord preparation from newborn rat. *Brain Res* **445**, 314–324.

Onimaru H & Homma I (2003). A novel functional neuron group for respiratory rhythm generation in the ventral medulla. *J Neurosci* **23**, 1478–1486.

Onimaru H, Kumagawa Y & Homma I (2006). Respiration-related rhythmic activity in the rostral medulla of newborn rats. *J Neurophysiol* **96**, 55–61.

Orem J & Brooks EG (1986). The activity of retrofacial expiratory cells during behavioral respiratory responses and active expiration. *Brain Res* **374**, 409–412.

Paton JF (1996). A working heart–brainstem preparation of the mouse. *J Neurosci Methods* **65**, 63–68.

Paton JF, Abdala AP, Koizumi H, Smith JC & St-John WM (2006). Respiratory rhythm generation during gasping depends on persistent sodium current. *Nat Neurosci* **9**, 311–313.

Peever JH, Mateika JH & Duffin J (2001). Respiratory control of hypoglossal motoneurones in the rat. *Pflugers Arch* **442**, 78–86.

Phillipson EA (1974). Vagal control of breathing pattern independent of lung inflation in conscious dogs. *J Appl Physiol* **37**, 183–189.

Pickering AE & Paton JF (2006). A decerebrate, artificially-perfused in situ preparation of rat: utility for the study of autonomic and nociceptive processing. *J Neurosci Methods* **155**, 260–271.

Richter DW (1982). Generation and maintenance of the respiratory rhythm. *J Exp Biol* **100**, 93–107.

Richter DW (1996). Neural regulation of respiration: rhythmogenesis and afferent control. In *Comprehensive Human Physiology*, ed. Gregor R & Windhorst U, pp. 2079–2095. Springer-Verlag, Berlin.

Rybak IA, Abdala AP, Markin SN, Paton JF & Smith JC (2007). Spatial organization and state-dependent mechanisms for respiratory rhythm and pattern generation. *Prog Brain Res* **165**, 201–220.

Shen LL, Li YM & Duffin J (2003). Inhibitory connections among rostral medullary expiratory neurones detected with cross-correlation in the decerebrate rat. *Pflugers Arch* **446**, 365–372.

Sherrey JH, Pollard MJ & Megirian D (1988). Proprioceptive, chemoreceptive and sleep state modulation of expiratory muscle activity in the rat. *Exp Neurol* **101**, 50–62.

Simms AE, Paton JFR, Pickering AE & Allen AM (2009). Amplified respiratory–sympathetic coupling in neonatal and juvenile spontaneously hypertensive rats: does it contribute to hypertension? *J Physiol* **587**, 597–610.

Smith JC, Abdala AP, Koizumi H, Rybak IA & Paton JF (2007). Spatial and functional architecture of the mammalian brain stem respiratory network: a hierarchy of three oscillatory mechanisms. *J Neurophysiol* **98**, 3370–3387.

Smith JC, Butera RJ, Koshiya N, Del Negro C, Wilson CG & Johnson SM (2000). Respiratory rhythm generation in neonatal and adult mammals: the hybrid pacemaker-network model. *Respir Physiol* **122**, 131–147.

Smith JC, Greer JJ, Liu GS & Feldman JL (1990). Neural mechanisms generating respiratory pattern in mammalian brain stem–spinal cord in vitro. I. Spatiotemporal patterns of motor and medullary neuron activity. *J Neurophysiol* **64**, 1149–1169.

Song G & Poon CS (2009). Lateral parabrachial nucleus mediates shortening of expiration during hypoxia. *Respir Physiol Neurobiol* **165**, 1–8.

Song G, Yu Y & Poon CS (2006). Cytoarchitecture of pneumotaxic integration of respiratory and nonrespiratory information in the rat. *J Neurosci* **26**, 300–310.

St-John WM, Zhou D & Fregosi R (1989). Expiratory neural activities in gasping. *J Appl Physiol* **66**, 223–231.

Strohl KP, Mead J, Banzett RB, Loring SH & Kosch PC (1981). Regional differences in abdominal muscle activity during various maneuvers in humans. *J Appl Physiol* **51**, 1471–1476.

Taccola G, Secchia L & Ballanyi K (2007). Anoxic persistence of lumbar respiratory bursts and block of lumbar locomotion in newborn rat brainstem spinal cords. *J Physiol* **585**, 507–524.

Tian GF, Peever JH & Duffin J (1999). Botzinger-complex, bulbospinal expiratory neurones monosynaptically inhibit ventral-group respiratory neurones in the decerebrate rat. *Exp Brain Res* **124**, 173–180.

Wittmeier S, Song G, Duffin J & Poon C-S (2008). Pacemakers handshake synchronization mechanism of mammalian respiratory rhythmogenesis. *Proc Natl Acad Sci U S A*, **105**, 18000–18005.

Zoccal DB, Simms AE, Bonagamba LG, Braga VA, Pickering AE, Paton JF & Machado BH (2008). Increased sympathetic outflow in juvenile rats submitted to chronic intermittent hypoxia correlates with enhanced expiratory activity. *J Physiol* **586**, 3253–3265.

Acknowledgements

This study was supported by the National Institute of Neurological Disorders and Stroke (NINDS), NIH grant R01 NS057815 and in part by the Intramural Research Program of the NIH, NINDS. J. F. R. Paton is the recipient of a Royal Society Wolfson Research Merit Award.